RRH: BROWN ANOLE EVOLUTION

PHYLOGEOGRAPHIC AND MORPHOGEOGRAPHIC OUTCOMES OF BROWN ANOLE COLONIZATION ACROSS THE CARIBBEAN PROVIDE INSIGHT INTO THE BEGINNING STAGES OF AN ADAPTIVE RADIATION

R. Graham Reynolds[1], Jason J. Kolbe[2], Richard E. Glor[3], Marta López-Darias[4], C. Verónica Gómez Pourroy[5], Alexis S. Harrison[5], Kevin de Queiroz[6], Liam J. Revell[7,8], and Jonathan B. Losos[9]

[1]*Department of Biology, University of North Carolina Asheville, One University Heights, Asheville, NC 28804, USA. Author for correspondence: E-mail: greynold@unca.edu; URL: http://www.caribbeanboas.org*

[2] *Department of Biological Sciences, University of Rhode Island, Kingston, RI 02881, USA*

[3] *Herpetology Division, Biodiversity Institute and Department of Ecology and Evolutionary Biology, University of Kansas, Lawrence, Kansas 66045, USA*

[4] *Island Ecology and Evolution Research Group, IPNA-CSIC, San Cristóbal de La Laguna, 38206, Tenerife, Canary Islands, Spain*

[5] *Department of Organismic and Evolutionary Biology, Harvard University, 26 Oxford St., Cambridge, MA 02138, USA*

[6] *Department of Vertebrate Zoology, National Museum of Natural History, Smithsonian Institution, Washington, DC 20560, USA*

[7] *Department of Biology, University of Massachusetts Boston, Boston, MA, 02125, USA*

[8] *Departamento de Ecología, Facultad de Ciencias, Universidad Católica de la Santísima Concepción, Concepción, Chile*

[9] *Department of Biology, Washington University in Saint Louis, Missouri, 63130, USA.*

Abstract (336 words); Text (11819 words); Acknowledgements (244 words); References (185 count; 4801 words); Tables (5); Figures (9); Supplementary information (16 Figures, 7 Tables)

Abstract.—

Some of the most important insights into the ecological and evolutionary processes of diversification and speciation have come from studies of island adaptive radiations, yet relatively little research has examined how these radiations initiate. We suggest that *Anolis sagrei* is a candidate for understanding the origins of the Caribbean *Anolis* adaptive radiation and propose that detailed investigation into the morphological and genetic variation of this widespread species can provide significant insight into how a colonizing anole species begins to undergo allopatric diversification, phenotypic divergence, and, potentially, speciation. To investigate the extent of diversification across *A. sagrei*, the most widespread of all anole species, we undertook a genetic and morphological analysis of representative populations across the entire native range of the species. We obtained mtDNA sequence data for 298 individuals from 95 locations and genomic data (31,702 SNPs for 69 of these individuals from 58 localities), which we analyzed using phylogenetic and population genetic methods. We also generated a morphometric dataset including 10 linear and meristic variables obtained from radiographs and photographs from 558 specimens. We find that *A. sagrei* originated in the early Pliocene, with the deepest divergence occurring between western and eastern Cuba. Lineages from these two regions subsequently colonized a large portion of the northern Caribbean, with some evidence for multiple colonization of regions such as the Bahamas and natural colonization of Jamaica. We find that at the broadest scale, populations colonizing areas with fewer closely related competitors tend to evolve larger body size and more lamellae on their toepads. This trend follows expectations for a convergence-shift scenario, whereby populations freed from competition with close relatives evolve towards common morphological and ecological optima. Taken together, our results show a complex history of ancient and recent Cuban diaspora on competitor-poor islands evolving

away from Cuban populations regardless of phylogenetic contingency, thus providing insight into the original diversification of colonist anoles at the beginning of the radiation. Our research also supplies an evolutionary framework for the many studies of this increasingly important species in ecological and evolutionary research.

KEY WORDS: Adaptive radiation, Caribbean, ecological release, genotyping-by-sequencing, morphometrics, next-generation sequencing, population genomics, phylogeography, convergent evolution?

Dedication: This manuscript is dedicated to the memory of Lourdes Rodríguez-Schettino, a remarkable scientist and major contributor to the systematics and ecology of Cuban anoles, including A. sagrei. Without her the present work (and so much else) would not have been possible.

Interest in adaptive radiation has increased greatly over the last two decades (Parent and Crespi 2009; Glor 2010; Losos and Mahler 2010; Yoder et al. 2010; Stroud and Losos 2016). Over a slightly longer period, the study of geographic variation, also known as phylogeography, has similarly expanded (Avise 2009; Knowles 2009). In many respects, these two areas of investigation are complementary. Research on adaptive radiation focuses on speciation and ecological diversification (Schluter 2000; Glor 2010; Yoder et al. 2010; Losos 2011a), whereas phylogeography focuses on intraspecific differentiation through geographic space (Avise 2000).

Most phylogeographic work focuses on patterns of genetic divergence among populations, though the adaptive basis of phenotypic differentiation is also occasionally studied (e.g., Deagle et al. 2013; Thorpe et al. 2015; Thorpe 2017). Relatively few projects unite these two perspectives; however, it is reasonable to suppose that in many cases adaptive radiations are initiated by the geographic divergence of populations. A phylogeographic perspective should thus provide important insights on the origins of adaptive radiation.

Understanding the early stages of adaptive radiation is often difficult, especially for old and diverse radiations for which little information regarding ancestral taxa survives. Especially on islands, a species in an adaptive radiation might bud off colonizing populations that occupy areas allopatric from other members of the radiation (Carlquist 1974). In this context, studying such populations might serve as a good analogue to the ancestral species that first colonized the islands, thus providing us with important insight into the earliest stages of adaptation and speciation that ultimately led to the radiation of the group (Grant 1998). The ecological release or ecological opportunity hypotheses also suggests that populations colonizing areas with fewer competitors should exhibit greater morphological trait variance than populations of the same species found in multi-species communities (Nosil and Reimchen; Bolnick et al. 2007; Yoder et al. 2010). Alternatively, populations might evolve directionally away from ancestral populations, owing to either idiosyncratic local selective pressures producing trait divergence among populations (i.e. Price et al. 2010) or general ‘relaxation’ towards a phenotypic optimum that is favored in the absence of competition resulting in similar phenotypic outcomes among populations (Lister 1976b).

Caribbean *Anolis* lizards are well-known for their replicated adaptive radiations on the islands of the Greater Antilles (reviewed in Williams 1969, 1972; Schluter 2000; Losos 2009), on which anole lineages have diversified ecologically and morphologically by specializing to use different microhabitats (Jackman et al. 1997; Losos et al. 1998; Mahler et al. 2013). A key feature of these replicated radiations is that almost all species are each confined to a single island. That is to say, the radiations are independent because there has been almost no recent exchange of species between islands (at least prior to human activity [Helmus et al. 2014]). These radiations, however, are quite old. The most recent molecular divergence-time estimates suggest that anoles may have begun diversifying around 50 million years ago (Poe et al. 2017; Román-Palacios et al. 2018). Given that the oldest known fossil anoles date to about twenty million years before the present (Sherratt et al. 2015), we have little direct evidence about the early stages of the Greater Antillean anole radiations, shrouded as they have been by the depths of time. Phylogenetic analysis makes it clear that anoles are descended from an ancestral mainland taxon, some of whose descendants later diversified on the islands of the Greater Antilles. But the ecological morphology of that colonizing species is hard to infer owing to the enormous quantity of time that has elapsed and to the evolutionary lability of traits associated with anole ecomorphs, leading in turn to low confidence in ancestral reconstructions (Losos 2011b; but see Losos and de Queiroz 1997; Poe et al. 2007).

The evolution of multi-species communities is not a one-way street: some species that evolved in multi-species anole communities in the Greater Antilles have subsequently colonized smaller islands where very few or no other anole species occurred (Losos et al. 1994; Losos and de Queiroz 1997; Poe et al. 2007). Species that occur on one- or two-species islands in the Lesser Antilles tend to have larger body sizes and more toepad lamellae (Losos and de Queiroz 1997;

Knox et al. 200; Poe et al. 2007), traits associated with arboreality in West Indian anoles (Williams 1983; Irschick et al. 2006). Furthermore, half a century ago Ernest Williams noted that, in contrast to the insular endemism that characterizes anole replicated radiations, four anole clades in particular are widespread and relatively adept at colonizing over water (Williams 1969). He noted that two species complexes, "*A. carolinensis*" (more accurately *A. porcatus*) and *A. sagrei*, are especially capable in this regard (Fig. 1a) and suggested that much could be learned about anole evolutionary diversification via study of these two taxa. If co-occurrence with close relatives leads species to occupy and adapt to specialized microhabitats, then subsequent colonization of depauperate communities might be expected to reverse this trend.

The most thorough test of Williams' hypothesis remains Lister's (1976a, b) examination of seven populations of *A. sagrei* across its range. Lister found that on islands with few or no other anole species, *A. sagrei* perched higher off the ground than the other semi-terrestrial "trunk-ground" habitat specialists of the Greater Antilles. Correspondingly, these populations evolved better-developed toepads (more lamellae), a trait that is linked to greater arboreality in anoles (Irschick et al. 2006). Despite the enormous amount of research devoted to anoles in the subsequent 40 years (Losos 2009), only a few studies have been focused on the diaspora of either of these two prolifically colonizing taxa (Kolbe et al. 2004; Glor et al. 2005), as well whether or not colonizing lineages of either taxon might have evolved under a scenario of ecological release (increased phenotypic variance) or directionally (divergent or convergent selection in different populations) when freed from competitive interaction with congeners (or trophically similar species; Wright 1981).

We aim to rectify this deficiency, focusing on *A. sagrei*, the most widely distributed currently recognized anole species in the Caribbean (Fig. 1b). Although *A. sagrei* is a workhorse in both ecological and evolutionary research programs (e.g., Cox and Calsbeek 2015; Driessens et al. 2015; Bonneaud et al. 2016; Delaney and Warner 2016; Fleishman et al. 2016; Logan et al. 2016; Schoener et al. 2017; Stroud et al. 2017; Kamath and Losos 2018; Lapiedra et al. 2018), we previously lacked an understanding of the magnitude and geographic distribution of genetic and morphological diversity within this widespread species. From its ancestral origins in Cuba, *A. sagrei* has colonized the Bahamas Archipelago to the north and east, as well as the Cayman Islands, Jamaica (although human-assistance in this case is debated), the Swan Islands (nearly 500 km south of the western tip of Cuba), and the Atlantic versant of Honduras, Mexico, and Belize (Figs. 1b, 2a; not to mention several farther-flung human-assisted introductions). Almost everywhere that it occurs naturally (possibly with exception of less-preferred habitats in Cuba), *A. sagrei* is the most common anole, with densities in some places as high as one lizard per square meter (Schoener and Schoener 1980). In their ecology and morphology, members of this species are classic "trunk-ground" anoles (Williams 1969), whose major habitat includes broad structures low to the ground, such as tree trunks and boulders. In Cuba, where the species evolved as part of the Cuban anole radiation currently comprising at least 64 extant species (Williams 1969; Kolbe et al. 2004), *A. sagrei* occurs in complex communities that can include as many as ten other anole species adapted to different structural and microclimatic niches (Williams 1969; Rodríguez-Schettino 1999; Rodríguez-Schettino et al. 2010). By contrast, throughout much of the rest of its non-Cuban range, *A. sagrei* co-occurs with few or no other anole species. In the Bahamas, for example, it can often be found on single-species islets that can be as small as 10 m^2 (Schoener and Spiller 2010), as well as larger islands with 1–3 other anole

species (Buckner et al. 2012). This geographic dispersion of *A. sagrei* suggests several interesting questions, most generally, how many times have islands been colonized directly from Cuba? Williams' (1969) figure (reproduced here as Fig. 1a, perhaps not meant to be taken literally in its original presentation), suggested as many as 12 dispersal events from Cuba to other regions in the Caribbean, thus raising the possibility that contingency (and not just selection) might lead to varying evolutionary outcomes across these islands.

This extraordinary colonizing ability, combined with its great abundance and ability to thrive in many different habitats, suggests that *A. sagrei* might be a good model for the ancestor of the anole adaptive radiations (Williams 1969; Losos 2009). In this situation, as populations in the *A. sagrei* diaspora are released from intense interspecific competition, we might expect them to experience ecological release (Lister 1976a; Nosil and Reimchen 2005; Losos and de Queiroz 1997; Yoder et al. 2010; Wellborn and Langerhans 2015). Nevertheless, more nuanced outcomes are possible, and based on previous hypotheses related to evolution in West Indian anoles, we make four predictions of potential outcomes for populations descended from ancestors that occurred in multi-species communities but which now find themselves in a relatively species-poor guild (Williams 1969). (1) 'Trait Variance Expansion.' Island-colonizing populations might have evolved greater morphological variance, potentially owing to selection favoring increased niche breadth related to ecological release/opportunity (e.g., Nosil and Reimchen 2005; Bolnick et al. 2010; but not seen in Lesser Antillean anoles [Eaton et al. 2002; Losos and de Queiroz 1997]). (2) 'Intraspecifc Expansion.' Island-colonizing populations might have evolved directionally away from the immediate ancestral morphology. Specifically, intraspecific diversification expands because individual populations experience idiosyncratic (directional) selective pressures owing to environmental heterogeneity on islands (e.g. Lister 1976a; Price et

al. 2010; Yoder et al. 2010). (3) 'Convergence.' Island-colonizing populations might evolve directionally towards a phenotypic optimum in the absence of competitors that differs from that of the progenitor population existing in an environment with congeneric competitors (Lister 1976b; Losos et al. 1998). (4) 'Evolutionary Contingency.' Island-colonizing populations might show no clear patterns of morphological diversification variation owing to differences in the evolutionary history of each island lineage and the relative ages of each population (e.g., Price et al. 2000). Here we examine these possible and not necessarily mutually-exclusive scenarios in *A. sagrei* across the complete native range of the species.

Materials and Methods

PHYLOGEOGRAPHY: GENETIC SAMPLE COLLECTION AND DATA

New genetic samples in this study represent collections spanning the last two decades by the authors and others. Our sampling of 298 individuals covered the range of *A. sagrei*, with between one and five samples from each of 95 localities across the northern Caribbean basin, including the Greater Antillean islands of Cuba (53 localities) and Jamaica (8 localities); the Great and Little Bahama Banks (9 localities); Cayman Islands (4 localities); Swan Islands (Islas de Cisne); and 15 localities on mainland Mesoamerica (Mexico, Belize, and Honduras) (Fig. 2a; Table S1). We also sampled other species closely related to *A. sagrei*, including *A. bremeri*, *A. quadriocellifer*, and *A. homolechis* (all of which are members of the *A. sagrei* "series"; Cádiz et al. 2013; or the *Trachypilus* clade Poe et al. 2017).

To generate sequences for our samples which did not already have published data (e.g. some sequences from Kolbe et al., 2004) we extracted whole genomic DNA (gDNA) from tissue samples using the Wizard SV® Kit (Promega, Madison, WI) and subsequently stored extracts at -20°C. We used the polymerase chain reaction (PCR) to amplify a fragment of the mitochondrial genome (NADH subunit 2 [*ND2*]; primers from Macey et al. 1997; conditions in Revell et al. 2007). We sequenced PCR products in both directions on an automated sequencer (ABI 3730XL) at the Massachusetts General Hospital DNA Core Facility, Cambridge, MA. We assembled contigs and visually verified ambiguous base calls using GENEIOUS® 7.1.2 (Biomatters, Auckland, New Zealand). We then generated an alignment including additional outgroups using the CLUSTALW 2.1 (Larkin et al. 2007) algorithm implemented in GENEIOUS using reference sequences and default parameters. We deposited this alignment in Dryad (accession # pending).

We analyzed the complete mtDNA dataset using both maximum likelihood (ML) and Bayesian methods. We selected the best-fit model of molecular evolution for the *ND2* locus (*TrN+G*) using the Bayesian information criterion (BIC) in JMODELTEST2 (Guindon and Gascuel 2003; Darriba et al. 2012). We conducted ML analysis using RAxML (Stamatakis 2006) via the RAxML plugin for GENEIOUS 7.1.2. We used the GTRGAMMA model, as the TrN model is not implemented in the software and the use of the invariant sites parameter (I) has been recommended against in RAxML (since RAxML, like all phylogeny inference software, implements a discretized Γ model, invariant sites is usually confounded with one of the Γ rate categories; Stamatakis 2006). We used the rapid bootstrapping algorithm with 10^3 bootstrap (BS) replicates followed by the thorough ML search option with 100 independent searches. We consider BS values above 95% to indicate well-supported clades and values ≥ 70% but < 95% to

indicate moderately supported clades (Felsenstein 2004; Taylor and Piel 2004). To generate rough estimates of divergence times across the mitochondrial gene tree, we inferred a time-calibrated *ND2* tree in the program BEAST v2.1.2 (Bouckaert et al. 2014). We estimated this tree using a relaxed molecular clock model and a rate of molecular evolution (1.3% pairwise divergence per million years) estimated via geologic events in related agamid lizards (Macey et al. 1998) that has been widely used in other studies of anoles (e.g., Creer et al. 2001; Jackman et al. 2002; Glor et al. 2003, 2004, 2005; Tollis et al. 2012; Campbell-Staton et al. 2013; Gartner et al. 2013). We relied on this estimated rate of pairwise divergence because few pre-Pleistocene fossil records exist for *Anolis*, and the small handful of specimens of amber-preserved anoles are either taxonomically ambiguous, making their placement on a phylogeny problematic (Castañeda et al. 2014), or are not very closely related to *A. sagrei* (Sherratt et al. 2015). We ran BEAST for 100 million generations using the *TrN+G* substitution model, a Yule speciation prior, and an uncorrelated lognormal (UCLN) relaxed molecular clock model. We repeated the analyses three times sampling every 10^4 generations and discarding the first 25% of generations as burn-in following analysis of likelihood trace files. All computations were conducted on the Odyssey cluster supported by the Harvard FAS Research Computing Group (odyssey.fas.harvard.edu). We assured adequate mixing of the chains by calculating the effective sample size (ESS) values for each model parameter, with ESS values greater than 200 taken to indicate adequate sampling of the posterior distribution. We assessed convergence of the independent runs by a comparison of likelihood scores and model parameter estimates in TRACER v1.5 (Rambaut et al. 2013). We combined the results from the three analyses using LOGCOMBINER and generated a maximum clade credibility (MCC) tree using TREEANOTATOR. We estimated genetic distances (Tamura-Nei [TrN] distances) between major clades using MEGA 6.0 (Tamura et al. 2013).

To examine nuclear diversity and divergence in the *A. sagrei* series, we selected a subset of 61 *A. sagrei* individuals representing each of the 11 main mtDNA clades identified in the previous analyses above and spanning the entire range of the species. We selected a further eight individuals of closely related taxa (*A. bremeri* n = 4, *A. quadriocellifer* n = 2, *A. homolechis* n = 2) that were also represented in our mtDNA dataset. We conducted GBS (genotyping-by-sequencing) using the nextRAD (Nextera®-tagmented reductively-amplified DNA) GBS approach as implemented by SNPsaurus (Institute of Molecular Biology, Eugene, OR, USA) followed by single nucleotide polymorphism (SNP) genotyping for these 69 samples from 58 localities. Briefly, nextRAD uses selective primers to amplify fragments across the genome, as opposed to using restriction enzymes followed by size selection (Baird et al. 2008; Etter and Johnson 2012). These fragments are initially generated using Illumina® Nextera® tagementation, followed by selective PCR amplification and ligation of sequencing adapters and barcoded indices (Russello et al. 2015). Prior to library preparation, we quantitated each of our gDNA samples using a Qubit® 2.0 fluorometer system. Genomic DNA was fragmented using the Nextera reagent (Illumina®, Inc.), which also ligates short adapter sequences to the ends of each fragment. This reaction calls for 15ng of gDNA per sample, though 22.5ng of gDNA were included to compensate for degraded DNA in some of our older samples. We then amplified these fragments using a selective primer complementary to the adapter sequences, which also includes a nine base-pair (bp) selective sequence (GTGTAGAGC). We conducted amplification using PCR at 73°C for 26 cycles, during which only fragments of gDNA that were able to hybridize with the selective sequence are amplified. We performed sequencing on an Illumina® NextSeq 500 at the Institute of Molecular Biology, Eugene, OR using a high-output run to generate ~400 million single-end sequencing reads 75bp in length. We? initially quality-filtered

our sequencing reads using Trimmomatic (Bolger et al. 2014) to remove adapters and low quality reads (with a Phred score of <20), resulting in a mean of 4,178,671 reads per individual. We called SNPs using the SNPsaurus nextRAD pipeline. This pipeline consists of custom scripts (SNPsaurus, LLC) that create a *de novo* reference from abundant reads. All sequencing reads are then mapped to the reference with an alignment identity threshold of 93% (BBMAP, http://sourceforge.net/projects/bbmap/). We called genotypes using SAMTOOLS and BCFTOOLS using the following flags: (samtools mpileup –gu –Q 10 –t DP, DPR –f ref.fasta –b anolis.align_samples | bcftools call –cv - > anolis.vcf). We converted the resulting variant-call format (VCF) genotype file to subsequent input files using PDGSPIDER (Lischer and Excoffier 2012) after excluding loci with only missing data and non-polymorphic loci, as well as SNPs with Phred scores less than 10. This resulted in 31,702 polymorphic SNPs across 12,415 loci (1–21 SNPs per locus), with an average of 7.62% missing data across 69 genotypes of *A. sagrei* and outgroups.

We used the package VCFR (Knaus and Grünwald 2017) in RStudio v1.0.136 (RStudio Team 2016) running R v3.2.4 (R Development Team 2016) to import and convert our VCF file within the R environment. We first assessed the quality of the SNP dataset by examining the distribution of missing data and minor alleles, as well as the distribution of SNPs across the 75bp reads using the R package ADEGENET (Jombart 2008; Jombart and Ahmed 2011). We then calculated per-locus statistics including observed and expected heterozygosity (H_o and H_e) and F_{ST} to test for deviations from Hardy-Weinberg equilibrium and to characterize genetic differentiation of populations.

To quickly examine phylogenetic distances among individuals in our SNP dataset, we constructed a neighbor-joining (NJ) tree using the R package APE (Paradis et al. 2004, 2016) after parsing the data with the package PEGAS (Paradis 2010). We visualized the tree using the package ADEGENET (Jombart 2008; Jombart and Ahmed 2011). We next constructed a phylogenetic tree using the neighbor-net algorithm implemented in SPLITSTREE v.4.13.1 (Huson and Bryant 2006) to visualize a network of the SNP genotypes and assessed support among the major groups using 10^3 nonparametric bootstrap replicates.

Another approach to defining geographic evolutionary "groupings" is to detect the degree to which individual island populations, lineages within islands, or island groups, form natural clusters of evolutionarily related populations. To do this, we used two methods to examine clustering of individual SNP genotypes across *A. sagrei* sampling locations. First, we used a discriminant analysis of principal components (DAPC; Jombart et al. 2010) implemented in the R package ADEGENET (Jombart 2008). This method attempts to maximize genetic differentiation between groups and minimize variation within groups by clustering individual genotypes using a principal components transformation of the genetic data prior to discriminant analysis. We used a BIC approach to obtain the predicted number of clusters between $K = 1$ and $K = 20$ after retaining n-1 PCs while optimizing the assignment of individuals to groups. To perform the DAPCs, we selected the optimal number of PCs to generate the discriminant functions using *optim.a.score()* in ADEGENET with 10^3 replications. We used a hierarchical set of analyses to examine clustering across our dataset. Our initial analysis included all 69 genotypes (including nominally different species within the *A. sagrei* series). We followed this with independent substructure analyses until we no longer detected multiple clusters. We examined loading plots to ensure that a small number of loci were not contributing to discriminant function loading.

A more explicit population genetic (allele-frequency based) approach to clustering is the Bayesian clustering algorithm STRUCTURE (Pritchard et al. 2000), which uses an MCMC approach to cluster *K* groups based on individual allele frequencies. We trimmed our SNP dataset to include only the first SNP from each of the first 1,000 loci to retain only presumably independent loci for clustering analyses (Pritchard et al. 2000). We used the admixture model and 10 replications of $K = 1$ to $K = 10$, with each replication consisting of a run length of 10^6 generations and a burn-in of 25% following evaluation of convergence. We selected values of *K* using the ΔK method of Evanno et al. (2005) implemented in STRUCTURE HARVESTER (Earl and vonHoldt 2012) and we visualized output using STRUCTURE PLOT (Ramasamy et al. 2014) after using the CLUMPP 1.1.2 (Jakobsson and Rosenberg 2007) algorithm to combine results across independent runs. As with DAPC, we used a hierarchical set of analyses to examine natural evolutionary clusters, or groups, across our dataset. Our initial run consisted of the full 61 genotype SNP dataset representing *A. sagrei* individuals from each of the mtDNA clades A–K (excluding the eight individuals representing other *A. sagrei* series species). Following this preliminary clustering, we subsequently ran nested substructure analyses as above.

We calculated Cavalli-Sforza and Edwards Chord Distance (*Dch*; Takezaki and Nei 1996), and Nei's Distance (*Ds*; Nei 1972) for each of the genomic groupings delimited in the above DAPC clustering analyses using the R package HEIRFSTAT (Goudet 2005). We tested for isolation-by-distance (IBD) in the *A. sagrei* SNP dataset (61 genotypes) by calculating pairwise *Dch* genetic distances between samples grouped by sampling locations in HEIRFSTAT. We converted sampling locations from latitude/longitude coordinates (decimal degrees) to log-transformed Euclidean distance measures using the GEOGRAPHIC DISTANCE MATRIX GENERATOR v1.2.3 (Ersts 2017). We then used ADEGENET (Jombart 2008; Jombart et al. 2011) to test the

hypothesis of IBD by computing matrix correlations (Mantel test; Mantel 1967) between the matrices using the *mantel.rtest()* function from the R package ADE4 (Dray and Dufour 2007) with alpha = 0.05 and 10^4 repetitions. We also conducted IBD analyses on the mtDNA data from the same individuals used to generate the SNP dataset. We reduced the mtDNA alignment to these individuals and calculated genetic distances among them in HEIRFSTAT using the *Ds* (Nei distance) model as a measure of minimum distances. We then conducted IBD analysis as above with the same geographic distance dataset.

To investigate whether a correlation exists between mitochondrial genetic distance and nuclear genomic distance, as might be expected given a strong phylogeographic signal (implicating allopatric diversification), we conducted a multiple-matrix regression (MMR) analysis (partial Mantel test) controlling for geographic distance. We used the function *mantel.partial()* in the R package VEGAN (Legendre and Legendre 2012; Oksanen et al. 2014) to model the SNP distance dataset as the dependent matrix, and the geographic and mtDNA distance datasets as the independent matrices using a Pearson coefficient and 10^3 permutations. We calculated genetic distances and geographic distances as above, and simultaneously visualized the matrices using the *surf3D()* function in the R package PLOT3D (Soetaert 2013).

MORPHOGEOGRAPHY: QUANTITATIVE TRAIT DIVERSIFICATION

Our scenarios for trait evolution in diasporic *A. sagrei* posit that we might see one or more of the following patterns : an expansion of trait variance within populations, a shift in trait values among populations (with populations evolving idiosyncratically or convergently or both), or no

apparent pattern of trait evolution owing to evolutionary contingency. To assess the evolution of presumably ecologically-relevant quantitative morphological traits (QTs) in *A. sagrei*, we examined 558 museum specimens representing 40 sampling locations across the range of the species for which we also had genetic data. We measured intact and well-prepared individuals (e.g., no missing limbs, body proportions undistorted by preservation) in the collection of the Harvard Museum of Comparative Zoology (MCZ), with supplemental loans from the Museum of Vertebrate Zoology at Berkeley (MVZ), the University of Kansas Biodiversity Institute (KU), the Natural History Museum of Los Angeles (NHMLA), and the Florida Museum of Natural History (FLMNH) (Table S2). To reduce potential complications owing to sexual dimorphism, we selected only adult males, ascertaining this condition by the presence of two or more of the following characteristics: an enlarged dewlap, a relatively wide tail base, everted hemipenes, enlarged post-anal scales, and a lack of typical female dorsal color pattern. We obtained a radiograph of each individual using a Thermo Kevex cabinet X-ray system (Model PX510-16W) at the MCZ, with a setting of 30μa and 30kV and a standard metric ruler on the detector plate. We taped each specimen to the detector plate to ensure that we obtained a consistent plane of focus, and we conducted image acquisition with VARIAN IMAGE VIEWING AND ACQUISITION (v2.0, Varian Paxscan Medical Systems). In addition, we scanned the toepads of each individual using a standard flatbed scanner (Epson v500) at a resolution of 1200–2600 dpi.

We analyzed both radiographs and scans in the program IMAGEJ 1.43 (Rasband, W.S., ImageJ, U. S. National Institutes of Health, Bethesda, Maryland, USA). A single observer (VGP) obtained the following nine linear measurements for each radiograph (Fig. S1): snout-vent length (SVL), head length from tip of rostrum to posterior of occipital (HL), head width behind the eyes (HW), snout width (SW), snout length (SL), upper jaw length (JL, average of left and right

sides), femur length (FL, average of left and right sides), tibia length (TL, average of left and right sides), and metatarsus length (MTL, average of left and right sides). We conducted symmetry and repeatability measurements on a subset of individuals to ensure reliability of the measurements, with the average for left- and right-side measurements being used after excluding specimens scored as asymmetric or unrepeatable (details in Gómez Pourroy 2014). We (RGR and VGP) counted lamellae on scanned images of the fourth hind toe using the multipoint function in IMAGEJ. We followed the methodology outlined in Köhler (2014), with the slight modification of counting lamellar scales from the distal to the proximal ends of phalanges II to IV of the fourth hind toe, beyond the plane of the basal joint where the fourth toe meets the third toe, to the last easily identifiable enlarged scale.

We log-transformed quantitative trait data to reduce skew and obtained residuals from a regression of each of the eight sets of linear measurements against SVL to control for overall size. We also size-corrected lamella counts, as body size and lamella number are potentially correlated in *Anolis* (Glossip and Losos 1997). We checked residuals for outliers and normality and used the residuals for subsequent analyses, taking the mean residuals for each sampling site. We performed these and all ensuing analyses in R, with a complete dataset consisting of the residuals of the nine linear measurements and counts. We initially surveyed the dataset for broad-scale (geographic) clustering in a multivariate framework using both *K*-means and model-based BIC clustering analyses which we implemented in the R package MCLUST (Fraley and Raftery 2002; Fraley et al. 2012).

We next used principal components analysis (PCA) implemented in R to determine whether morphological variation in our nine-character QT dataset is partitioned among Cuban

anoles and their diaspora. We used population mean residuals from size-correction and examined loadings, biplots, and proportion of explained variance to examine our ability to discriminate between these two groups. To test whether Cuban populations differed significantly from diaspora populations, we conducted MANOVA on all PC axes and then on residuals from a regression of all QTs on SVL, followed by tests for mean trait shifts using independent *t*-tests (Cuba versus diaspora) on each of the nine QTs with Benjamini-Hochberg correction (Benjamini and Hochberg 1995) for multiple tests. We calculated mean and variance of the size-corrected residuals for each trait grouped by Cuba or diaspora (Cuba n = 140; diaspora n = 420). Despite these groupings consisting of divergent evolutionary lineages (see below), we are interested in whether a reduction of sympatric anole species yields a detectable shift in morphological traits. We then used a Levene's test to test for trait variance expansion between Cuban and diaspora populations followed by visualizing the data using density plots in GGPLOT2 (Wickham 2009) in R.

Next, we assessed QT divergence within and among a series of *a priori* groupings to determine whether relationships exist between morphological variation and geographic/genetic/taxonomic grouping, or whether morphological variation is independent of prior grouping. We first repeated the above PCA with points colored-coded by broad geographic region (Bahamas, Cayman Islands, Cuba, Jamaica, Mesoamerica, and Swan Islands), to visualize among-group separation in morphometric space. We then assessed whether QTs were different among regional groupings using an ANOVA followed by *post-hoc* Tukey tests. To then explicitly test our ability to use morphometric data to discriminate among *a priori* groups, we conducted a linear discriminant function analysis using the *lda()* function in the R package MASS (Venables and Ripley 2002). This multivariate method maximizes variance among groups

specified *a priori*, rather than variance across the dataset (as in PCA). Our intention was to assess our ability to distinguish among groups defined by geographic region, genetic group (as identified in both the SNP and mtDNA datasets), and nominal subspecies. We fit models to various *a priori* groupings (*Cuba/diaspora*, *Region, mtDNA* group, *DAPC* group, *STRUCTURE* group, and *Subspecies*) against population means of size-corrected residuals from nine morphological measurements and assessed the intragroup variance represented by each discriminant function. We plotted the first two LD axes to visualize group discrimination. We then estimated our ability to use the discriminant axes to predict group membership for individual populations. To do so, we used the *predict()* function in the MASS package to generate predicted population assignments based on the LD axes. We then determined the proportion of times in which that population was correctly assigned to its prior grouping (proportion of correct assignments = PoCA). We followed this by using a 1-tailed exact binomial test to determine whether we were more successful than expected by chance in our ability to correctly reassign a population to a group based on LDA of QTs.

At such a broad geographic scale, morphological variation could simply be related to geographic distance ("morphological isolation-by-distance"). To investigate whether morphological diversification is correlated with geographic distance, we performed independent matrix correlation analyses (Mantel tests) between geographic distances and each of the first three PCs (which encompassed the majority of the variance) from the morphological dataset. We converted geographic distances from the latitude/longitude coordinates (decimal degrees) associated with the museum specimens to UTM coordinates using the *convUL()* function in the R package PBSMAPPING (Schnute et al. 2013). We then calculated pairwise Euclidean distance matrices from each of the orthogonalized PC axes and the log-transformed geographic distances.

We conducted Mantel tests as above using the *mantel.randtest()* function in the R package ADE4 (Dray and Dufour 2007) with 10^3 permutations.

To assess the possibility of evolutionary contingency, we tested phylogenetic signal in our QT dataset, we pruned our ultrametric Bayesian mtDNA tree to lineages for which we could obtain QT means for each tip. We then reconstructed continuously valued QT lineage means along the phylogenetic history of *A. sagrei* using the function *contMap()* in the R package PHYTOOLS (Revell 2012, 2013). We obtained residuals for each QT by fitting a phylogenetic regression against body size (SVL) using *phyl.resid()* in PHYTOOLS (Revell 2009). We tested for phylogenetic signal in each of the continuous traits by calculating Pagel's (1997, 1999) λ using *phylosig()* in PHYTOOLS to examine whether these QTs are evolving in concert with the phylogeny (λ close to zero implies that the trait is poorly correlated with the phylogeny and thus may be homoplastic). We conducted 10^3 Brownian motion simulations of the null hypothesis of homoplasy for each QT to generate *P* values for tests of phylogenetic signal.

Results

PHYLOGEOGRAPHY: GENETIC SAMPLE COLLECTION AND DATA

We generated an alignment of 1,101 bp for the mitochondrial *ND2* sequence data (full coding sequence plus 3' *tRNA-TRP*) from 298 *A. sagrei* series haplotypes, as well as individuals from the outgroups *A. homolechis*, *A. mestrei*, and *A. ophiolepis* which we obtained through both direct sequencing and from online sequence repositories (Table 1). Both Bayesian and ML analyses resulted in similar estimated topologies for the *ND2* gene tree (Dryad # forthcoming)

that were well supported (Fig. 2b). We collapsed the tree into 11 non-overlapping clades representing biogeographic breaks (Fig. 2b). As in previous studies (Kolbe et al. 2004, 2008; Cádiz et al. 2013), we found a main clade of *A. sagrei* haplotypes (clades A–J) distributed across the range of the species (Fig. 2a,b), as well as a sister clade (clade K) containing a mixture of *A. sagrei*, *A. quadriocellifer*, and *A. bremeri* haplotypes from western Cuba (Pinar del Río Province) with a tentative coalescent time (given that it is inferred from an approximate mtDNA clock rate of 0.65% per lineage per million years, and without any internal fossil calibration points) in the late Miocene or early Pliocene 6.4 Ma (BS = 87; PP = 0.42; 95% highest posterior density interval [HPD] 7.4 – 5.5 Ma). We hereafter refer to the inclusive clade composed of clades A–K as *A. sagrei* (*sensu lato*), while clades A–J represent *A. sagrei* (*sensu stricto*). The node subtending *A. sagrei sensu lato* and the outgroup *A. homolechis* had a coalescent time of 6.8 Ma (95% HPD 8.5 – 5.4 Ma). We found evidence for a coalescence between eastern (I and J) and western (A, B, C, and E) Cuban clades in the early Pliocene 5.2 Ma (BS = 96; PP =0.99; 95% HPD 5.9 – 4.5 Ma), with a contact zone east of Camagüey, Cuba.

Based on our tree topology, we inferred that subsequent dispersals from Cuba have given rise to other Caribbean populations (Fig. 2b, c). We found that the Bahamas contain two divergent, non-sister mtDNA clades (D and F), possibly resulting from independent colonization events from western Cuba (Fig. 2b). These clades are not partitioned by island bank: instead, clade D is represented on the western Great Bahama Bank (BS = 86; PP =1; 95% HPD 4.1 – 2.8 Ma), while clade F (BS = 51; PP =0.99; 95% HPD 5.4 – 4.2 Ma) is distributed on the eastern Great Bahama Bank, the Little Bahama Bank, and the southern Bahamas banks (San Salvador Bank and Crooked/Acklins Bank; Fig. 2b, c). We found evidence for a single dispersal to the Cayman Islands from East Cuba (BS = 92; PP =1; 95% HPD 4.1 – 2.9 Ma), with Cayman Brac

(clade G) and Little Cayman (clade H) populations being reciprocally monophyletic and moderately divergent sister clades (BS = 100; PP =1; 95% HPD 3.1 – 1.7 Ma).

Our Bayesian and ML analyses of the mtDNA data identified two distinct clades present in Mesoamerica, both of which are nested within the south Cuban clade (clade I; Fig. 2b, c; Fig. S2). The first clade contains haplotypes from Mesoamerica as well as Little Swan Island and is divergent from Cuban members of clade I with a coalescent time of 1.6 Ma (BS = 80; PP = 0.9; 95% HPD 1.8 – 1.3 Ma; Fig. S2). The Little Swan Island population is sister to a haplotype from Campeche, Mexico (BS = 97; PP = 1; 95% HPD 0.8 – 0.3 Ma), which together are distinct from a sister Mesoamerican clade (BS = 99; PP = 1; 95% HPD 1.4 – 0.8 Ma) consisting of 18 Mesoamerican haplotypes from Veracruz southeast to Honduras (including four other Campeche, MX haplotypes). The second Mesoamerican clade consists of only three haplotypes from Belize and Honduras, which are sister (BS = 82; PP = 1) to haplotypes from South Cuba (and western Jamaica). Great Swan Island is not sister to Little Swan Island (Fig. S2); instead it is represented by a separate clade nested within the South Cuba clade (I), albeit with low nodal support (BS = 49; PP = 1; 95% HPD 1.0 – 0.6 Ma).

Jamaica has haplotypes representing two divergent mtDNA clades (clades I and J), with the south Cuba clade I represented in the west and the east-central Cuba clade J represented in the east (Figs. S2, S3). Western Jamaican (clade I) haplotypes are interdigitated with, and minimally divergent from, Cuban haplotypes from the vicinity of Portillo (Fig. S2). Eastern Jamaican (clade J) haplotypes on the other hand form a monophyletic group (BS = 99; PP = 1) sister to two of four haplotypes from Vertientes, Cuba, with a coalescent time of 0.5 Ma (95% HPD 0.7 – 0.3 Ma; Fig. S3).

Genetic distances (Tamura-Nei [TrN] distances) between major mtDNA clades ranged from 6.1% pairwise divergence (Cayman Brac Clade G – Little Cayman Clade H) to 15.3% (Western Cuba Clade K – Western Bahamas Clade D; Table S3). We found a significant pattern of isolation-by-distance in the mtDNA dataset, although the correlation between genetic and geographic distance explained little of the variation ($r = 0.17$, $P = 0.001$; Table 2, Fig. 3a).

We used 31,702 polymorphic SNPs among 69 individuals to better characterize genetic structure of *A. sagrei* across the northern Caribbean. These SNPs were evenly distributed across the 75bp sequence reads (Fig. S4; average depth of sequencing 20x) and while some loci might be under selection, we found no evidence for bias attributable to a minority of loci (Fig. S5). Missing data and minor alleles were distributed evenly across the matrix of individuals and SNPs (Fig. S6), with an average of 6.5% missing data per-individual (mode = 2.6%) except for the two individuals of the outgroup *A. homolechis* (50% and 49% missing data, probably owing to a combination of sample degradation and lower orthology relative to filtered ingroup SNPs). While many alleles are nearly fixed across individuals, a large number occur at intermediate allele frequencies (Fig. S4). We found that observed heterozygosity (H_o) varied among loci (Fig. S7) and found a significant difference (Bartlett test of homogeneity of variances $K^2 = 91.22$, $P < 0.001$) between expected heterozygosity (H_e) and H_o on a per-locus basis (Fig. S8), just as we might expect due to population subdivision.

As in the mtDNA dataset, we found the deepest split in the nuclear genomic dataset occurring between East Cuba and West Cuba, as visualized by both an NJ tree (Fig. 2c) and a phylogenetic network (Fig. 4). We also found phylogenetic groupings concordant with the mtDNA dataset for other geographic regions, with the Cayman Islands representing a highly

divergent split from the rest of *A. sagrei* (minimum *Ds* = 0.16; Table S4). Contrary to our results from mtDNA, we found that Bahamas lineages represent a clade separate from those in western Cuba (minimum *Ds* = 0.18; Table S4). Western Cuba has a series of clades that are discordant with the mtDNA phylogeographic breaks. One individual identified as *A. quadriocellifer* in our mtDNA tree (USNM 515920) belongs to the West Cuba lineage of *A. sagrei* (Figs. 2, 4). The Mesoamerican and Swan Island populations are sister to each other, and unlike in our mtDNA tree, are reciprocally monophyletic. As in the case with the mtDNA tree, these clades are nested with the smallest clade containing all of the South Cuba samples (Fig. 2c).

Our Δ*K* analysis on STRUCTURE runs of 1,000 SNP loci among 61 *A. sagrei* genotypes (Table 3) resulted in an initial partitioning of East Cuba (plus the Cayman Islands, Swan Islands, and Mesoamerica) and West Cuba (plus the Bahamas) at *K* =2, followed by the next likely clustering of *K* = 4 separating East Cuba, West Cuba, the Cayman Islands, and the Bahamas (Fig. 5a; Fig. S9). Within the West Cuba group (20 genotypes), we found two clusters, separating the Bahamas from Cuba (Fig. 5a; Fig. S9). We also found two clusters in the East Cuba group (34 genotypes), separating South Cuba, the Swan Islands, and Mesoamerica from east-central Cuba and Jamaica (Fig. 5a), though most of these populations show some representation (assignment uncertainty possibly due to admixture) from both genetic clusters (Fig. S9). The next likely clustering for the East Cuba cluster is *K* = 5, which separates out geographic regions into clusters— the Swan Islands, South Cuba (admixed), Mesoamerica, Jamaica (admixed), and east-central Cuba (two samples admixed). In both cluster-sets, Jamaica appears to be admixed between east-central Cuban lineages (Fig. S9), as predicted by mtDNA, and some admixture between these lineages is apparent on Cuba as well, suggesting gene flow between these regions.

Discriminant analyses implemented in DAPC were largely congruent with STRUCTURE clustering (Table 3; Fig. 5; Figs. S10, S11). For the initial analysis including both *A. sagrei* and other members of the *A. sagrei* series (*A. bremeri*, *A. quadriocellifer*, *A. homolechis*), we obtained $K = 5$ (retaining 5 PCs) composed of Bahamas, West Cuba, East Cuba, Cayman Islands, and other *A. sagrei* series species (Fig. 5b; Figs. S10, S11). One sample(of two) of *A. quadriocellifer* was found to cluster with the Western Cuba group, and individuals from the East Cuba-West Cuba contact zone grouped with the East Cuba cluster. For the next analysis, we included only *A. sagrei sensu stricto* samples, obtaining $K = 3$ (retaining 2 PCs) composed of West Cuba, East Cuba (including contact zone individuals), and the Cayman Islands. For the West Cuba group, we found $K = 4$ (retaining 3 PCs), discriminating West Bahamas, north-east Bahamas, West Cuba, and west-central Cuba. Within the East Cuba group, we found $K = 3$ (retaining 2 PCs), distinguishing east-central Cuba plus Jamaica (no inferred admixture in Jamaica), South Cuba (plus the Swan Islands), and Mesoamerica. We did not find evidence for discriminant functions being obviously driven by loadings of a small number of loci (Fig. S12).

We found genetic distances (Cavalli-Sforza Chord and Nei's D) ranging from 0.05 (South Cuba – Swan Islands – east-central Cuba) to 0.34 – 0.36 (Cayman Islands – West Bahamas) among major genetic clusters of *A. sagrei* (Table S4). Other *A. sagrei* series species (*A. homolechis*, *A. quadriocellifer*, and *A. bremeri*) are all highly divergent from *A. sagrei sensu stricto*, although they exhibit lower divergence from western Cuba *A. sagrei* samples. *Anolis quadriocellifer* had relatively smaller genetic distances to western Cuba *A. sagrei* and we found that at least one of the individuals (USNM 515920) that appears to have *A. quadriocellifer* mtDNA haplotype but a nuclear genome most similar to western Cuba *A. sagrei*, suggesting an explanation for lower inferred genetic distance if gene flow between these species has occurred.

We found a significant pattern of isolation-by-distance in the SNP dataset (r = 0.38, *P* = 0.001; Table 2; Fig. 3b). This strong effect of geographic distance on genomic variation is in contrast with the weaker geographic effect on mtDNA distances (r = 0.17, *P* = 0.001; Table 2; Fig. 3a). Geographically neighboring mtDNA haplotypes are not necessarily characterized by low mtDNA divergences across the range of *A. sagrei* (Fig. 3d). Multiple matrix regression indicated a significant effect of mtDNA distance on genomic distance, controlling for geographic distance (r = 0.58, *P* = 0.001, Table 2).

MORPHOGEOGRAPHY: QUANTITATIVE TRAIT DIVERSIFICATION

We obtained complete QT data (consisting of SVL plus nine residuals from linear measurements regressed against SVL) from 558 individuals representing each of the major genetic groups found in this study (per-group mean n = 51.2; range n = 17 – 134), an adequate population-level sample size for characterizing major morphological traits such as body size (Stamps and Andrews 1992). We did not detect any outliers and the data were normally distributed. Analyses of mean and variance on a trait-by-trait basis for Cuban populations and diaspora populations showed an increase in mean SVL and lamellar count, as well as an increase in trait variance for SVL, head width, and femur length in diasporic populations (Table 4; Fig. 6).

While we found between 2–4 non-differentiated "clusters" across the entire dataset by examining the within-group sum of squares from a *K*-means clustering analysis (Fig. S13), and two clusters from our BIC clustering analysis ("VVE" model; Fig. S14), these clusters overlapped extensively in morphospace. Visualization of the clusters in the space defined by the

first two PC axes (75.6% of the variation) from our model-based BIC clustering analysis indicated a lack of clustering by genetic or geographic grouping in PC space (Figs. S13, S14). In PCA morphospace generated from our nine QTs, we found that diaspora populations tended to disassociate from Cuban populations on PC axis 1 (Fig. 7a), an axis associated with size-corrected lamella number. Principal components axes 2 and 3, on which loaded snout size and leg length, respectively, showed little differentiation between Cuban and diaspora populations (Table S5). Our MANOVA suggested ready differentiation between Cuban and diaspora groupings based on all nine PC axes, and our individual *t*-tests showed that this is largely driven by differences in SVL ($t = 6.24$, $P < 0.001$; Table 4) and size-corrected lamella number ($t = -6.53$, $P < 0.001$; Table 4). When we further examined QTs we found that they differed significantly among groups (Cuba, Bahamas, Caymans, Mesoamerica, Swan Islands) in an ANOVA analysis (Table 4) and further that all diaspora groups were significantly different from Cuban populations in at least two QTs or more (Fig. S15), with diaspora groups evolving larger body size and more lamellae (Fig. 8). In addition, most diaspora groups were different with respect to each other in a number of QTs (Fig. S15).

Our LDA approach also allowed us to readily distinguish Cuban from diaspora lizards on a single LD axis (Fig. 7b). Our estimate of group prediction based on LD axes suggested a 93% probability of correct group reassignment for either population based on LD1 ($P < 0.001$; Table 5). When we overlaid geographic regions (Cuba, Bahamas, Cayman Islands, Mesoamerica, Swan Islands) onto the PCA morphospace, we saw that some regional diaspora groupings were especially well differentiated from Cuban populations and, to some extent each other, owing largely to differences in lamella number, which loads heavily on PC1 (Fig. 9a). Our ANOVA analyses showed significant differences among some geographic groups for all QTs (Fig. S15).

LDA generated some additional predictive assignment ability based on QTs. Our LDA indicated that most traits contribute to discrimination along LD axis 1 and/or LD axis 2 (Table S6), though leg length (TL, FL) is strongly predictive of *a priori* geographic groupings among analyses. For the geographic region grouping, LD1 loaded with head shape traits (SW, SL, JL, HW) and lamella number, and readily differentiated between Cuban and diaspora regional groups, whereas leg length loaded strongly on LD2 and differentiated Mesoamerican and Swan Island populations from other regions (Table S6; Fig. 9). Our LD axes further demonstrated strong ability to discriminate among *a priori* geographic groupings (Fig. 9b; Table 5), with an 88% probability of correct reassignment (PoCA), far higher than expected by chance ($P < 0.001$). We also found this method correctly assigns individuals to their groups for all other *a priori* groupings (*Subspecies* = 90%, *DAPC* = 80%, *STRUCTURE* = 85%, *mtDNA* = 85%) with much higher probabilities than expected by chance (Table 5).

We found a low, yet significant, correlation between geographic distance and morphological distance, as represented by the first orthogonal axis from our PCA analysis (Table 2; Fig. S16). We found evidence of phylogenetic signal ($\lambda > 0$) only for SVL ($\lambda = 0.42$, $P = 0.008$), suggesting that other morphological traits, such as more lamellae in diasporic populations, are largely homoplastic and do not reflect shared evolutionary history (Table S7).

Discussion

While interspecific studies of Caribbean lizards have advanced our understanding of macro-scale evolutionary processes such as adaptive radiation (Poe et al. 2017; Losos 2009), intraspecific

studies of Caribbean *Anolis* biogeography and phylogeography can provide insight into what might have unfolded during the early stages of diversification of a group. In particular, we posit that careful study of intraspecific genetic and morphological variation within widespread anole species can reveal a great deal about the pattern and process of evolutionary divergence (Glor et al. 2003; Rodríguez-Robles et al. 2007; Thorpe et al. 2008, 2010; Ng and Glor 2011; Glor and Laport 2012; Muñoz et al. 2013; Wollenberg et al. 2013). Species that have colonized previously anole-free islands thus may serve as a model for early stages of adaptive radiation, analogous to the original species of anole or anoles that reached the Caribbean. We tested four possible, though not mutually exclusive, scenarios for how colonizing populations of *A. sagrei* have evolved morphologically following expansion from Cuba.

MORPHOGEOGRAPHY OF A COLONIZING SPECIES

Trait Variance Expansion Scenario

The underlying rationale for a prediction of ecological release is that populations occurring largely without the competition of close relatives should expand their resource use to take advantage of resources used by other species in multi-species communities (i.e., "ecological opportunity" [Yoder et al. 2010; Wellborn and Langerhans 2015; Stroud and Losos 2016]), and that subsequently populations should evolve to be more morphologically variable because morphologically different individuals will use different components of the resource spectrum. Our data provide some evidence for increased morphological variance in SVL, head width, and femur length (Fig. 6), suggesting that increased ecological niche breadth in *A. sagrei* (Lister 1976a; reviewed for anoles in Losos 2009) is potentially accompanied by increased

morphological variability (though we emphasize that our samples are modest relative to ideal estimates of variance). An alternative mechanism for niche expansion involves the evolution of increased morphological and ecological sexual dimorphism (e.g., Bolnick and Doebeli 2003). We cannot test this hypothesis with our data as the majority of museum samples are of male anoles and this is also what we focused our sampling on.

Intraspecific Expansion Scenario

Morphological evolution in diasporic populations might proceed under the suggested ecological release scenario (Schoener 1969; Lister 1976a,b), whereby anoles colonizing islands with few other anole species experience relaxed competition with closely related taxa and are thus subject to different selective regimes. Such a scenario can result in trait variance expansion but could also produce an expansion of intraspecific morphospace when populations on different islands evolve directionally in separate directions from ancestral populations (e.g. Price et al. 2010).

We found a weak (but significant) correlation between morphological distance and geographic distance across the northern Caribbean. In other words, morphological distances might be explained, at least in part, by geographic distance, as neighboring populations are more morphologically similar than distant populations. While this morphology-by-distance relationship does not translate into distinctly clustered morphological groups under any of the *a priori* groupings, such as *Region* (Fig. 9), we are still able to diagnose populations based on multivariate analysis of QTs with high confidence (Table 5). This suggests that there are some idiosyncratic evolutionary outcomes in diasporic populations. While most diaspora are evolving directionally in PC morphospace relative to Cuban populations (Figs. 7–9), our ability to detect

differences among populations suggests that traits are evolving differently in different populations. Further, our ANOVA analyses and post-hoc tests (Table 4; Fig. S15) demonstrate that population pairs have evolved along independent trajectories for some QTs but not others. Taken together, these observations suggest that, while we see some concerted shifts in morphospace among diasporic populations, we also are able to detect idiosyncratic morphological evolution and general support for some intraspecific expansion of morphospace owing to colonization of different islands.

Convergence Scenario

Lister (1976a, b) found that on islands with diasporic *A. sagrei* but few or no other anole species, *A. sagrei* perched higher and evolved more lamellae, suggesting that colonizing lineages might be convergent with regard to these traits (owing to common selective pressures, such as competitive release). We greatly expanded upon Lister's sampling and find results that support his conclusions plus the extension of determining that the populations are evolutionarily independent. *Anolis sagrei* populations on outlying islands — the result of 4–5 evolutionary dispersals (see below) — have consistently evolved in the same direction (including larger body size and more lamellae) relative to Cuban populations remaining in the ancestral range (Figs. 6–9), and Cuban *A. sagrei* are morphologically distinguishable in a LDA analysis from those of the diaspora (LD1 = 100%; Fig. 7; Table 5). It is known that some ecologically important morphological characteristics can evolve rapidly in anoles (Stuart et al. 2014; Winchell et al. 2016), and some diasporic populations are characterized by "extreme" traits (relative to other *A. sagrei*) along some morphological axes (body size, lamella number, dewlap color; Fig. 8).

Furthermore, these traits—increased body size and increased number of lamellae—are associated with increased arboreality in West Indian anoles (Irschick et al. 2006).

It is worth noting that on the islands of the Lesser Antilles, a number of species—members of the *bimaculatus* and *roquet* species groups—occur alone and that the evolutionary trends evidenced by *A. sagrei* are in the direction of being more like these species in having larger body sizes (Losos and de Queiroz 1997; Poe et al. 2007) and more toepad lamellae (Losos and de Queiroz 1997; Knox et al. 2001). These repeated patterns suggest that solitary occurrence (i.e. a lack of congeners) might favor particular morphological traits, at a? minimum, larger overall body size and higher lamella numbers if not other characteristics. Of particular note, our samples from Jamaica, which represent a diasporic population, do not differ morphologically from Cuban samples (Fig. 9). This is further evidence that it is the presence of other anole species (six additional species on Jamaica), and not other factors, that has acted to curb evolutionary trait shifts in *A. sagrei*.

Evolutionary Contingency Scenario

If morphological divergence is only weakly related to geographic distance, as our data show, another non-mutually exclusive hypothesis is that morphology might be correlated with the evolutionary history of populations encoded in phylogeny. Our data show precisely the opposite: phylogeographic relationships based on information from organellar genomes indicates that the evolution of phenotypic similarity among diasporic lineages has no relationship to the reconstructed evolutionary history of the different populations in this study (i.e., we found no

indication of phylogenetic signal for nine QTs, and only limited signal for SVL; Table S7). That populations on the Cayman Islands, Bahamas, and Swan Islands—all with different source populations and thus evolutionary backgrounds—would be convergent along some phenotypic axes suggests that this situation likely owes to selective pressures for these traits on anole-depauperate islands (Lister 1976b). This interpretation is further supported by our finding of a lack of difference in Jamaican populations, which experience a similar competitive environment to Cuban lizards. While we find no evidence for phylogenetic signal on a trait-by-trait basis (except for SVL), variance components among traits (discriminant axes) appear sufficient to predict evolutionary relationships using morphological data (Table 5). Thus, in a multivariate context, intergroup variance components allow us to predict genetic or geographic group membership using discriminant axes (Table 5). This suggests that genetic and geographic group membership imparts a consistent pattern to morphological traits. Natural selection appears to be driving similar phenotypic outcomes in populations with different evolutionary histories, but multivariate analysis can detect idiosyncrasies, such as collective morphological shifts, among groups.

EVOLUTIONARY HISTORY: COLONIZATION AND PHYLOGEOGRAPHY

Here we have attempted to reconstruct patterns of diaspora for *A. sagrei* by focusing on region-by-region evolutionary and phylogeographic history. Taken together, our data suggest between four and five dispersal events from Cuba, leading to the populations presently found on the Bahamas Islands, Cayman Islands, Jamaica, and Mesoamerica. We address each below.

Origins and evolution of Cuban Anolis sagrei

Our genetic data suggest two important patterns in *A. sagrei sensu stricto* on the island of Cuba. First, the mtDNA shows a Miocene split between the eastern and western portions of the island (HPD 5.9 – 4.5 Ma), with a present "contact" zone east of Camagüey (Fig. 2a). While we note that our estimates of inferred coalescent time must naturally pre-date (and thus overestimate) the actual time of lineage separation (Degnan and Rosenberg 2009), this timing of coalescence is consistent with the suggested separation of Cuba into a western paleoisland and central+eastern archipelago in the Miocene (Iturralde-Vinent and MacPhee 1999; Graham 2003; Iturralde-Vinent 2003, 2006). This finding is congruent with evolutionary reconstructions of other Cuban taxa demonstrating an east-west split (5.0 Ma, Glor et al. 2004; 5.8 Ma, Alonso et al. 2012), and is also a common phylogenetic feature in many other intraspecific studies of Cuban terrestrial fauna (e.g., Weiss and Hedges 2007; Rodríguez et al. 2010; Matos-Maraví et al. 2014). Phylogeographic structure in the form of deep mtDNA coalescence is an increasingly common finding in anole species (Malhotra and Thorpe 2000; Glor et al. 2004; Knouft et al. 2006; Cádiz et al. 2013; Geneva et al. 2015), possibly owing to local adaptive differentiation in some cases (Irwin 2012; Thorpe et al. 2015).

Analysis of our genomic SNP dataset reveals many of the same phylogeographic patterns in Cuba suggested by mtDNA, although we find that the east/west contact zone shifts northwestward by about 150 km to the vicinity of Sancti Spiritus province. That this deep east-west split within *A. sagrei* is evinced by both organellar and nuclear genomes indicates that it likely represents a historical break, rather than deep coalescence combined with IBD. Such a pattern might, for example, owe to ancestral populations evolving in allopatry for a period of

time on Cuban paleoislands. The latter would suggest a separation subsequent to the inundation of central Cuba following the formation of the Havana-Matanzas channel (Iturralde-Vinent and MacPhee 1999; Iturralde-Vinent 2003). This seems unlikely given that the reconnection of east and west Cuba is thought to have occurred in the Miocene and thus would pre-date the age of the inferred split in *A. sagrei*. A focused study of central Cuba and the evolutionary history of the *A. sagrei* series (*A. sagrei*, *A. homolechis*, and *A. mestrei*) might clarify this question.

Other *A. sagrei* clades on Cuba are likely derived from paleogeographic processes operating throughout the evolutionary history of the species. For example, Clade E is of more recent derivation, consistent with the later emergence of the Zapata Peninsula in the Pleistocene (Iturralde-Vinent 2003), close to where this clade was found (although we lack samples from the peninsula itself). Undoubtedly contact zones between lineages are dynamic through time, though geographically coherent groups such as Clade E (Fig. 2b) are consistent across some other taxonomic groups (e.g., Alonso et al. 2012).

Origins of Jamaican Anolis sagrei

Anolis sagrei is commonly thought to be anthropogenically introduced to Jamaica and some islands off of Mesoamerica (Williams 1969; Nicholson et al. 2012; Helmus et al. 2014). Based on historical records, it seems that *A. sagrei* was present in localized areas on Jamaica prior to 1850 (Gosse 1850 [“*Draconura catenata*”]; Lynn and Grant 1940; Underwood and Williams 1959; Crombie 1999). Kolbe et al. (2004) demonstrated that Jamaican *A. sagrei* most likely represents two independent colonizations from eastern Cuba, at least one of which might have

been human-assisted. Our analyses found a similar pattern, with two distinct mtDNA clades represented on the island. Eastern Jamaica has east-central Cuba haplotypes (mtDNA clade J), while western Jamaica has South Cuba haplotypes (clade I). We find that eastern Jamaican haplotypes (east-central Cuban affinities) form a divergent clade (Fig. S3), with an mtDNA coalescent time of 0.5 Ma (95% HPD 0.3 – 0.7 Ma), suggesting that this population may be the result of a geologically recent natural colonization event. In contrast, western Jamaican haplotypes are interdigitated with haplotypes extant in the vicinity of Portillo, Cuba (Fig. S2) and is thus likely to be of recent, anthropogenic origin. While our sampling is not dense enough to determine an exact contact zone between these two lineages on Jamaica, it appears to be in either Manchester or Clarendon Parish in the south. Our genomic data also suggest two introductions to the island from these Cuban source populations, though no distinct contact zone is discernible at our level of sampling, and Jamaican individuals are likely admixed in the nuclear genome (based on STRUCTURE results; Fig. S9), suggesting interbreeding on the island. Such a situation is unsurprising given apparent admixture of these lineages in the native Cuban range (Fig. S9) and the propensity of introduced *A. sagrei* lineages to interbreed (Kolbe et al. 2008, 2017). Given these data, we suggest that *A. sagrei* on Jamaica likely resulted from the combination of an initial natural dispersal from east-central Cuba and a more recent human-facilitated introduction from south Cuba. Our nuclear genetic data suggest that these two lineages are probably interbreeding and expanding their ranges, and hence are not likely to remain separate over the long term. We suggest that this artificial secondary contact would be a very interesting subject for further study.

Origins of Caymanian and Bahamian Anolis sagrei

The Cayman Islands have two morphologically divergent populations of *A. sagrei* (Kolbe et al. 2017). The population on Cayman Brac, the easternmost island in the Cayman Islands, has long been recognized as either a subspecies (*A. s. luteosignfer*; Ruibal 1964) or a species (*A. luteosignifer*; Garman 1888; Nicholson et al. 2012; Uetz and Hošek 2016), and is thought to be of ancient origin (e.g., Poe 2004; Henderson and Powell 2009). Individuals on Cayman Brac have relatively small dewlaps that range from rusty yellow to pale orange to red, either with or without a light margin. In contrast, *A. sagrei* on Little Cayman (7.5 km west of Cayman Brac) have very large red dewlaps with a light margin and hence have always been referred to as *A. s. sagrei*. Our genetic data show that these Caymanian lineages (excluding Grand Cayman, which harbors an introduced population; Kolbe et al. 2017) are highly divergent from other populations of *A. sagrei* (3.5 Ma minimum? coalescent time; minimum Ds = 0.18; Table S4; Figs. 2,3,4,5). In addition, Cayman Brac and Little Cayman haplotypes form sister clades with an estimated mitochondrial coalescent time of 2.4 Ma (95% HPD 3.1 – 1.7 Ma), suggesting that these lineages have been separated since the early Pleistocene. Genomic data also support a single origin for Little Cayman and Cayman Brac populations (Fig. 1; Figs. S7–S9).

Populations in the Bahamas are currently recognized as *A. s. ordinatus*, and our results are mixed with regard to the origins of this group, demonstrating the importance of deploying nuclear and organellar genetic data. Our mtDNA tree strongly suggests two colonizations of the Bahamas from western Cuba, one of the eastern and southern Bahamas <4.8 Ma and a second of the western Bahamas approximately 3.4 Ma (Fig. 2b). Deep mtDNA branches suggest that populations on isolated banks (San Salvador, Crooked Island) have persisted for some time (Dryad accession #tbd), in spite of some prior suggestions to the contrary (Schwartz 1968). Our nuclear genomic data suggest a single colonization from western Cuba (*Ds* = 0.08; Table S4;

Figs. 2c, 4). This latter result is striking, as the Great Bahamas Bank was recently a single, fully emergent island at the height of the last glaciation (~15,000 years ago), and a number of previous studies have assumed that populations on the Great Bahama Bank constitute a single genetic lineage (Calsbeek and Smith 2003; Calsbeek et al. 2007). In our results, both nuclear and mtDNA markers suggest an east-west split across the Bahamas. The presence of more than one mtDNA lineage could reflect separate colonizations of the Bahamas from Cuba, though the nuclear data do not support this (Fig. 2c). Alternatively, the mtDNA data might reflect incomplete lineage sorting. Morphological data suggest that at a coarse-scale, Bahamian lineages are relatively diverse—occupying, for example, the majority of the range of all *A. sagrei* specimens for LD1 (Fig. 9b); and individual island populations are known to exhibit a large degree of morphological differentiation (Losos et al. 1994; Vanhooydonck et al. 2009; Marnocha et al. 2011; Driessens et al. 2017).

Origins of Mesoamerican and Swan Island Anolis sagrei

Mesoamerican *A. sagrei* are presently recognized as a subspecies (*A. s. mayensis*; Smith and Burger 1949), implying a natural origin (Williams 1969; Schwartz and Thomas 1975), though evidence of introduced populations exists for the Bay Islands off the coast of Honduras (McCranie et al. 2005; Harrison 2014; McCranie and Köhler 2015). The type specimen of this subspecies is from Campeche, Mexico (Smith and Burger 1949; Cochran 1961); hence many authors treat Mexican and Belizean populations as *A. s. mayensis*, while Honduran populations are of unknown affiliation (e.g., Sexton and Brown 1977; Lee 2000; Kraus 2009). Mesoamerican populations are generally characterized by larger body size (Lee 1992; Fig. 8), and Swan Island

865 *A. sagrei* (presently considered *A. s. nelsoni*; Ruibal 1964) have the largest SVL of any *A. sagrei* populations (Lee 1992; Fig. 8). We found that Mesoamerican populations probably represent natural occurrences of the species on the mainland, derived from one or more overwater colonization events from south Cuba sometime in the mid- to late Pleistocene (Fig. 2b; Fig. S2). One of these colonization events likely also seeded Little Swan Island (Fig. S2). Our finding of 870 one Belizean and two Honduran mainland haplotypes as nested within a separate clade of South Cuban, Jamaican, and Big Swan haplotypes may suggest a second dispersal to Mesoamerica (Williams 1969; Fig. S2).

The Swan Islands, located between Honduras and the Cayman Islands, contain populations of *A. sagrei* that are highly distinctive from others in having a dark dewlap, unique 875 dorsal coloration, and body sizes far exceeding that of any other *A. sagrei* population (Lister 1976b; Harrison 2014; McCranie and Köhler 2015; Fig. 8). These populations have long been considered by some to be a separate species, *A. nelsoni* (Barbour 1914; Nicholson et al. 2012; McCranie and Köhler 2015), yet little was known regarding their phylogenetic affiliation with other *A. sagrei* populations. Our data show that Swan Island anoles are not deeply divergent 880 from South Cuba animals (Ds = 0.05; Table S4), and we were minimally successful in finding natural clusters for Mesoamerican and Swan Island individuals based on allele frequency data (Figs. S7–S9). Genomic data suggest a single colonization, possibly from Mesoamerica. Nevertheless, Mesoamerica and the Swan Islands display unique allele frequencies, suggesting sufficient time since colonization for selection and drift, which might be strong given the small 885 size of the Swan Islands, to act upon both the genomes and the phenotypes of the anoles of this site.

Surprisingly, Little Swan Island and Big? Swan Island haplogroups are not sister in either the Bayesian or ML mtDNA analyses (Fig. S2). It is unclear what to make of this, given that the two islands are separated by a breaking shoal less than 250 m wide and 10 m deep. Our genomic dataset suggests that Mesoamerican and Swan Island individuals form reciprocally monophyletic sister lineages (Figs. 2c, 4), which points to a single colonization of these regions from Cuba and supports relationships inferred in previous studies using morphological data (Lee 1992). A likely explanation for the origin of the Swan Island organellar and nuclear inconsistencies might be lineage sorting, owing to sampling and founder effects generating consistent yet divergent haplotypes on the two islands, naturally subsampled from the diverse southern Cuba clade via overwater dispersal.

AN EVOLUTIONARY BACKGROUND FOR A MODEL SPECIES

For such an important species in studies of ecology, behavior, and evolutionary biology as *A. sagrei*, it is surprising that little was known regarding its range-wide variation in genetics and morphology. Here we have provided a comprehensive macro-scale reconstruction of the evolutionary history of *A. sagrei*, as well as the breadth of morphological diversity in this species.

Comparative studies of *A. sagrei* populations have addressed a wide variety of questions, including how populations respond to colonization, how populations conform to predictions from island biogeographic theory, the evolutionary and ecological outcomes of founder effect, how geography influences dewlap color, the relationship between behavior and natural selection,

among many others (Schoener and Schoener 1983; Losos et al. 1997; Vanhooydonck et al. 2009; Kolbe et al. 2012; Lapiedra et al. 2018). However, our finding of the deep phylogenetic structure highlight the importance of investigating phylogeographic relationships within widespread species. Particularly striking in this regard is our finding that *A. sagrei* of the Bahamas are composed of two distinct and divergent evolutionary lineages. Most comparative studies of Bahamian populations (e.g., Losos et al. 1994) have not incorporated phylogeographic information (as none was available for these populations). The findings of these prior studies may warrant re-examination in the light of our newfound knowledge.

For example, by examining microsatellite allele frequencies across island populations, Calsbeek and Smith (2003) and Calsbeek et al. (2007) suggested that hurricanes mediate adaptive diversification by influencing directional gene flow across the Bahamian Tongue of the Ocean. This has been influential in our understanding of the effect of gene flow on intraspecific adaptive diversification not only in lizards (e.g., de Queiroz 2005; Glor et al. 2005), but also in other vertebrate taxa (e.g., Stankiewicz et al. 2006; Yoder and Nowak 2006), as well as in biogeography more generally (e.g., Dayan and Simberloff 2005; Garant et al. 2007; Riddle et al. 2008). We now know (as the authors of these studies could not have) that the populations compared in these studies come from two divergent clades that appear to coalesce 4 Ma before the present. Given the antiquity of the clades and issues of homoplasy with microsatellites (Anmarkrud et al. 2008), one might question whether seemingly identical alleles in the different clades are in fact homologous. Re-examination of the genetic relationships with other markers, analyzed in the context of phylogenetic relationships, would be desirable.

CONCLUSIONS

In the context of intraspecific diversification, our data show a pattern of morphological evolution consistent with the predictions of an ecological release scenario across a variety of phylogenetic contexts and evolutionary timescales. Across the broad range of *A. sagrei*, we are seeing a species leaving a species-rich ecological context and undergoing morphological evolution on species-poor islands. Our analyses suggest that diaspora undergo morphological shifts relative to Cuban progenitor populations, leading in some cases to similar morphological outcomes (increased lamella number, large body size) as well as a general expansion of the morphospace of the species. This occurs despite a wide range of evolutionary histories for these diasporas, originating from one or the other of two deeply divergent progenitor lineages (East Cuba vs. West Cuba) and with millions of years of differences between colonization events. Thus, we find support for three of our four predicted scenarios: colonizing populations of *A. sagrei* evolve increased trait variance and experience directional and convergent evolution for some traits (SVL, lamellae) relative to Cuban and Jamaican populations in multi-species communities. We argue that *A. sagrei* represents a potential example of how a colonizing *Anolis* species might seed Caribbean islands to begin the process of adaptive radiation—but essentially in reverse to the initial diversification of the West Indian *Anolis*.

SUPPLEMENTARY MATERIAL

We have archived phylogenetic trees and other associated data in Dryad (doi forthcoming). R code to replicate analyses presented herein will be available from GitHub (https://github.com/caribbeanboas).

FUNDING

We are grateful for funding from the Putnam Fund for Research and Exploration from the Museum of Comparative Zoology and the John Templeton Foundation. We are also grateful for funding from the National Museum of Natural History Research Opportunities Fund (to KdQ), National Museum of Natural History Biological Diversity Program (to KdQ), the National Science Foundation (#9318642 to JBL, KdQ, and A. Larson), and Tenerife 2030 (P. INNOVA 2016–2021; MLD). Additional support was also provided by Harvard University, the Museum of Comparative Zoology, the National Museum of Natural History, the University of North Carolina Asheville, the University of Califrand the University of Massachusetts Boston.

ACKNOWLEDGMENTS

All samples were collected with generous permission and permitting from the following agencies: Bahamas Environment, Science, and Technology Commission, Bahamas National Trust, Richard Belisle of the Office of the Deputy Prime Minister and Ministry of Natural Resources of Belize, Cayman Islands Department of Environment, Andrea Donaldson of the Natural Resources Conservation Authority of Jamaica, the Dirección General de Recursos

Naturales Renovables of Honduras, and Lourdes Rodríguez-Schettino, Naomi Cuervo Pineda, and Pedro Pérez Alvarez of the Instituto de Ecología y Sistematica, Academia de Ciencias de Cuba. A special thank you to Lourdes Rodríguez-Schettino who facilitated fieldwork in Cuba. The authors are grateful to the following individuals for assistance with fieldwork: Molly Morris, Leo Fleishman, Marguerite Butler, Duncan Irschick, Lourdes Rodríguez-Schettino, Ada Chamizo, and Todd Jackman. We thank Levi Gray and Steve Poe for loaning four genetic samples from Mexico. We also thank Adrián Nieto Montes de Oca (UNAM) for donating samples from Mexico. We thank Breda Zimkus for loaning samples through the Museum of Comparative Zoology Cryogenic Collection, and Jim Hanken and José Rosado for collection access. We thank Anthony Geneva and Raphaël Scherrer for some R code and assistance related to LD analyses, as well as Christian Lehner for assistance with some measurements. We further thank members of the Losos, Kolbe, Reynolds, and Revell labs for useful discussions and insight related to this project. We finally thank participants of the 7th *Anolis* Symposium held at Fairchild Tropical Botanical Gardens for comments on this project.

LITERATURE CITED

Alonso, R., A. J. Crawford, and E. Bermingham. 2012. Molecular phylogeny of an endemic radiation of Cuban toads (Bufonidae: *Peltophryne*) based on mitochondrial and nuclear genes. J. Biogeogr. 39:434–451.

Anmarkrud, J. A., O. Kleven, L. Bachmann, and J. T. Lifjeld. 2008. Microsatellite evolution: mutations, sequence variation, and homoplasy in the hypervariable avian microsatellite locus HrU10. BMC Evol. Biol. 8:138.

Avise, J. C. 2000. Phylogeography. Harvard University Press, Cambridge.

Avise, J. C. 2009. Phylogeography: retrospect and prospect. J. Biogeogr. 36:3–15.

Baird, N. A., P. D. Etter, T. S. Atwood, et al. 2008. Rapid SNP discovery and genetic mapping using sequenced RAD markers. PLoS One 3:e3376.

Barbour, T. 1914. A contribution to the zoogeography of the West Indies, with especial reference to amphibians and reptiles. Mem. Mus. Comp. Zool. 44:209–359.

Benjamini, Y., and Y. Hochberg. 1995. Controlling the false discovery rate: a practical and powerful approach to multiple testing. J. Royal Statist. Soc. Series B 57:289–300.

Bolger, A. M., M. Lohse, and B. Usadel. 2014. Trimmomatic: a flexible trimmer for Illumina sequence data. Bioinformatics 30:2114–2120.

Bolnick, D. I. and M. Doebeli. 2003. Sexual dimorphism and adaptive speciation: two sides of the same ecological coin. Evolution 57:2433-2449.

Bolnick, D. I., R. Svanback, M. Araujo, and L. Persson. 2007. More generalized populations are also more heterogeneous: comparative support for the niche variation hypothesis. Proc. Natl Acad. Sci. USA 104:10075–10079.

Bonneaud, C., E. Marnocha, A. Herrel, B. Vanhooydonck, D. J. Irschick, and T. B. Smith. 2016. Developmental plasticity affects sexual size dimorphism in an anole lizard. Funct. Ecol. 30:235–243.

Bouckaert, R., J. Heled, D. Kühnert, T. G. Vaughan, C-H. Wu, D. Xie, M. A. Suchard, A. Rambaut, and A. J. Drummond. 2014. BEAST2: A software platform for Bayesian evolutionary analysis. PLOS Comput. Biol. 10(4):e1003537.

Buckner, S. D., R. Franz, and R. G. Reynolds. 2012. Bahama Islands and Turks & Caicos Islands in R. Powell and R.W. Henderson, eds. Island lists of West Indian amphibians and reptiles. Bull. Florida Mus. Nat. Hist. 51:85–166.

Cádiz, A., N. Nagata, M. Katabuchi, L. M. Díaz, L. M. Echeniqu-Díaz, H. D. Akashi, T. Makino, and M. Kawata. 2013. Relative importance of habitat use, range expansion, and speciation in local species diversity of *Anolis* lizards in Cuba. Ecosphere 4:Article 78.

Calsbeek, R., and T. B. Smith. 2003. Ocean currents mediate evolution in island lizards. Nature 426:552–555.

Calsbeek, R., T. B. Smith, and C. Bardeleben. 2007. Intraspecific variation in *Anolis sagrei* mirrors the adaptive radiation of Greater Antillean anoles. Biol. J. Linn. Soc. 90:189–199.

Campbell-Staton, S. C., R. M. Goodman, N. Backstrom, S. V. Edwards, J. B. Losos, and J. J. Kolbe. 2013. Out of Florida: mtDNA reveals patterns of migration and Pleistocene range expansion of the Green Anole lizard (*Anolis carolinensis*). Ecol. Evol. 2:2274–2284.

Carlquist, S. 1974. Island Biology. Columbia University Press.

Castañeda, M. d. R., E. Sherratt, and J. B. Losos. 2014. The Mexican amber anole, *Anolis electrum*, within a phylogenetic context: implications for the origins of Caribbean anoles. Zool. J. Linn. Soc. 172:133–144.

Cochran, D. M. 1961. Type specimens of reptiles and amphibians in the U.S. National Museum. Bull. U.S. Nat. Mus. 220:xv–289.

Cox, R. M., and R. Calsbeek. 2015. Survival of the fattest? Indices of body condition do not predict viability in the brown anole (*Anolis sagrei*). Funct. Ecol. 29:404–413.

Creer, D. A., K. de Queiroz, T. R. Jackman, J. B. Losos, and A. Larson. 2001. Systematics of the *Anolis roquet* series of the southern Lesser Antilles. J. Herpetol. 35:428–441.

Crombie, R. I. 1999. Jamaica. Pp. 63–92 *in* B. I. Crother, ed. Caribbean Amphibians and Reptiles Academic Press, San Diego, CA.

Darriba, D., G. L. Taboada, R. Doallo, and D. Posada. 2012. jModelTest 2: more models, new heuristics and parallel computing. Nature Methods 9:772.

Dayan, T., and D. Simberloff. 2005. Ecological and community-wide character displacement: the next generation. Ecol. Lett. 8:875–894.

de Queiroz, A. 2005. The resurrection of oceanic dispersal in historical biogeography. TRENDS Ecol. Evol. 20:68–73.

Deagle, B. E., F. C. Jones, D. M. Absher, D. M., Kingsley, and T. E. Reimchen. 2013. Phylogeography and adaptation genetics of stickleback from the Haida Gwaii archipelago

revealed using genome-wide single nucleotide polymorphism genotyping. Mol. Ecol. 22:1917–1932.

Degnan, J. H., and R. A. Rosenberg. 2009. Gene tree discordance, phylogenetic inference and the multispecies coalescent. TRENDS Ecol. Evol. 24:332–340.

Delaney, D. M., and D. A. Warner. 2016. Age-and sex-specific variations in microhabitat and macrohabitat use in a territorial lizard. Behav. Ecol. Sociobiol. 70:981–991.

Dray, S., and A. B. Dufour. 2007. The ade4 Package: Implementing the Duality Diagram for 439 Ecologists. J. Statistical Softw. 22(4).

Driessens, T., K. Huyghe, B. Vanhooydonck, and R. Van Damme. 2015. Messages conveyed by assorted facets of the dewlap, in both sexes of *Anolis sagrei*. Behav. Ecol. Sociobiol. 69:1251–1264.

Earl, D. A., and B. M. vonHoldt. 2012. STRUCTURE HARVESTER: a website and program for visualizing STRUCTURE output and implementing the Evanno method. Conserv. Genet. Res. 4:359–361.

Eaton, J. M., S. C. Larimer, K. G. Howard, R. Powell, and J. S. Parmerlee. 2002. Population densities and ecological release of the solitary lizard *Anolis gingivinus* in Anguilla, West Indies. Caribbean Journal of Science 38:27–36.

Ersts, P. J. 2017. [Internet] Geographic Distance Matrix Generator (version 1.2.3). American Museum of Natural History, Center for Biodiversity and Conservation. Available from http://biodiversityinformatics.amnh.org/open_source/gdmg. Accessed on 2017-1-15.

Etter, P. D., and E. A. Johnson. 2012. RAD paired-end sequencing for local de novo assembly and SNP discovery in non-model organisms. Pp. 135–151 *in* F. Pompanon and A. Bonin, eds. Data Production and Analysis in Population Genomics: Methods and Protocols. Humana Press, New York, New York.

Evanno, G., S. Regnaut, and J. Goudet. 2005. Detecting the number of clusters of individuals using the software STRUCTURE: a simulation study. Mol. Ecol. 14:2611–2620

Felsenstein, J. 2004. Inferring Phylogenies. Sinauer Associates, Sunderland, MA.

Fleishman, L. J., C. W. Perez, A. I. Yeo, K. J. Cummings, S. Dick, and E. Almonte. 2016. Perceptual distance between colored stimuli in the lizard *Anolis sagrei*: comparing visual system models to empirical results. Behav. Ecol. Sociobiol. 70:541–555.

Fraley, C., A. E. Raftery, T. B. Murphy, and L. Scrucca. 2012. mclust Version 4 for R: Normal Mixture Modeling for Model-Based Clustering, Classification, and Density Estimation Technical Report No. 597, Department of Statistics, University of Washington.

Fraley, C., and A. E. Raftery. 2002. Model-based clustering, discriminant analysis and density estimation. J. Am. Statistical Assoc. 97:611–631.

Garant, D., S. E. Forde, and A. P. Hendry. 2007. The multifarious effects of dispersal and gene flow on contemporary adaptation. Funct. Ecol. 21:434–443.

Garman, S. 1888. Reptiles and batrachians from the Caymans and from the Bahamas. Collected by Prof. C.J. Maynard for the Museum of Comparative Zoology at Cambridge, Mass. Bull. Essex Inst. 20:101–113.

Gartner, G. E. A., T. Gamble, A. Jaffe, A. Harrison, and J. B. Losos. 2013. Left–right dewlap asymmetry and phylogeography of *Anolis lineatus* on Aruba and Curaçao. Biol. J. Linn. Soc. 110:409–426.

Geneva, A. J., J. Hilton, S. Noll, and R. E. Glor. 2015. Multilocus phylogenetic analyses of Hispaniolan and Bahamian trunk anoles (*distichus* species group). Mol. Phylogenet. Evol. 87:105–117.

Glor, R. E. 2010. Phylogenetic insights on adaptive radiation. Ann. Rev. Ecol. Evol. Syst. 41:251–270.

Glor, R. E., and R. G. Laport. 2012. Are subspecies of *Anolis* lizards that differ in dewlap color and pattern also genetically distinct? A mitochondrial analysis. Mol. Phylogenet. Evol. 64:255–260.

Glor, R. E., J. J. Kolbe, R. Powell, A. Larson, and J. B. Losos. 2003. Phylogenetic analysis of ecological and morphological diversification in Hispaniolan trunk-ground anoles (*Anolis cybotes* group). Evolution 57:2383–2397.

Glor, R. E., M. E. Gifford, A. Larson, J. B. Losos, L. Rodríguez-Schettino, A. R. C. Lara, and T. R. Jackman. 2004. Partial island submergence and speciation in an adaptive radiation: a multilocus analysis of the Cuban green anoles. Proc. Roy. Soc. Lond. Biol. Sci. 271:2257–2265.

Glor, R. E., J. B. Losos, A. Larson. 2005. Out of Cuba: overwater dispersal and speciation among lizards in the *Anolis carolinensis* subgroup. Mol. Ecol. 14:2419–2432.

Glossip, D., and J. B. Losos. 1997. Ecological correlates of number of subdigital lamellae in Anoles. Herpetologica 53:192–199.

Gómez Pourroy, C. V. 2014. Lizards in Space! Biogeographic variation in morphometrics of *Anolis sagrei*. Master's Thesis, Ludwig-Maximilians Universität, München & Museum of Comparative Zoology, Harvard University.

Gosse, P. 1850. Description of a new genus and six new species of saurian reptiles. Ann. Magazine of Nat. Hist. VI:344–348.

Goudet, J. 2005. Hierfstat, a package for R to compute and test hierarchical F-statistics. Mol. Ecol. Notes 5:184–186.

Graham, A. 2003. Geohistory models and Cenozoic paleoenvironments of the Caribbean region. Syst. Bot. 28:378–386.

Grant, P. R. 1998. Evolution on Islands. Oxford University Press, New York.

Guindon, S., and O. Gascuel. 2003. A simple, fast and accurate method to estimate large phylogenies by maximum-likelihood. Syst. Biol. 52:696–704.

Harrison, A. S. 2014. The evolution and diversity of the *Anolis* dewlap. Doctoral Dissertation, Harvard University, pp. 191.

Helmus, M. R., D. L. Mahler, and J. B. Losos. 2014. Island biogeography of the Anthropocene. Nature 513:543–546.

Henderson, R.W., and R. Powell. 2009. Natural History of West Indian Reptiles and Amphibians. The University of Florida Press, Gainesville, FL.

Huson, D. H., and D. Bryant. 2006. Application of phylogenetic networks in evolutionary Studies, Mol. Biol. Evol. 23:254–267.

Irschick, D.J., A. Herrel, and B. Vanhooydonck. 2006. Whole-organism studies of adhesion in pad-bearing lizards: creative evolutionary solutions to functional problems. J. Comp. Physiol. A. 192:1169-1177.

Irwin, D. E. 2012. Local adaptation along smooth ecological gradients causes phylogeographic breaks and phenotypic clustering. Am. Nat. 180:35–49.

Iturralde-Vinent, M. A. 2003. Ensayo sobre la paleogeografía del Cuaternario de Cuba Memorias, resúmenes y trabajos.V Congreso de Geología y Minería, CD ROM, 74 pp. La Habana, Cuba.

Iturralde-Vinent, M. A. 2006. Meso-Cenozoic Caribbean paleogeography: Implications for the historical biogeography of the region. Int. Geol. Rev. 48:791–827.

Iturralde-Vinent, M. A. and R. D. E. MacPhee. 1999. Paleogeography of the Caribbean region: implications for Cenozoic biogeography. Bull. Am. Mus. Nat. Hist. 238:1–95.

Jackman, T. R., D. J. Irschick, K. de Queiroz, J. B. Losos, A. Larson. 2002. Molecular phylogenetic perspective on evolution of lizards of the *Anolis grahami* series. J. Exp. Zool. (Mol. Dev. Evol.) 294:1–16.

Jackman, T., J. B. Losos, A. Larson, and K. de Queiroz. 1997. Phylogenetic studies of convergent adaptive radiations in Caribbean *Anolis* lizards. Pp. 535–557 in T.J. Givnish and K.J. Sytsma, eds., Molecular Evolution and Adaptive Radiation. Cambridge University Press: Cambridge.

Jakobsson, M., and N. A. Rosenberg. 2007. CLUMPP: a cluster matching and permutation program for dealing with label switching and multimodality in analysis of population structure. Bioinformatics 23:1801–1806.

Jombart, T. 2008. adegenet: a R package for the multivariate analysis of genetic markers. Bioinformatics 24:1403–1405.

Jombart, T., and I. Ahmed. 2011. adegenet 1.3-1: new tools for the analysis of genome-wide SNP data. Bioinformatics 27:3070–3071.

Jombart, T., S. Devillard, F. Balloux. 2010. Discriminant analysis of principal components: a new method for the analysis genetically structured populations. BMC Genet. 11:94.

Kamath, A., and J. B. Losos. 2018. Estimating encounter rates as the first step of sexual selection in the lizard *Anolis sagrei*. Proc. R. Soc. B, 285 (1873):20172244.

Knaus, B. J., and N. J. Grünwald. 2017. VCFR: a package to manipulate and visualize variant call format data in R. Mol. Ecol. Res. 17:44–53.

Knouft, J. H., J. B. Losos, R. E. Glor, and J. J. Kolbe. 2006. Phylogenetic analysis of the evolution of the niche in lizards of the *Anolis sagrei* group. Ecology 87:S29–S38.

Knowles, L. L. 2009. Statistical phylogeography. Ann. Rev. Ecol. Syst. 40:593–612.

Knox, A.K., J.B. Losos, and C.J. Schneider. 2001. Adaptive radiation versus intraspecific differentiation: morphological variation in Caribbean *Anolis* lizards. J. Evol. Biol. 14:904–909.

Köhler, G. 2014. Characters of external morphology used in *Anolis* taxonomy– definition of terms, advice on usage, and illustrated examples. Zootaxa 3774:201–257.

Kolbe, J. J., R. E. Glor, L. Rodríguez-Schettino, A. C. Lara, A. Larson, and J. B. Losos. 2004. Genetic variation increases during biological invasion by a Cuban lizard. Nature 431:177–181.

Kolbe, J.J., A. Larson, J.B. Losos, and K. de Queiroz. 2008. Admixture determines genetic diversity and population differentiation in the biological invasion of a lizard species. Biol. Lett. 4:434–437.

Kolbe, J. J., M. Leal, T. W. Schoener, D. A. Spiller, and J. B. Losos. 2012. Founder effects persist despite adaptive differentiation: a field experiment with lizards. Science 335: 1086–1089.

Kolbe, J.J., J.E. Wegner, Y.E. Stuart, U. Milstead, K.E. Boronow, A.S. Harrison, and J.B. Losos. 2017. An incipient invasion of Brown anole lizards (*Anolis sagrei*) into their own native range in the Cayman Islands: a case of cryptic back-introduction. Biol. Inv. 19:1989–1998.

Kraus, F. 2009. Alien Reptiles and Amphibians. A Scientific Compendium and Analysis. Springer Science, New York.

Lapiedra, O., T. W. Schoener, M. Leal, J. B. Losos, and J. J. Kolbe. 2018. Predator-driven natural selection on risk-taking behavior in anole lizards. Science 360:1017–1020.

Larkin, M. A., G. Blackshields, N. P. Brown, R. Chenna, P. A. McGettigan, H. McWilliam, F. Valentin, I. M. Wallace, A. Wilm, R. Lopez, J. D. Thompson, T. J. Gibson, and D. G. Higgins. 2007. Clustal W and Clustal X version 2.0. Bioinformatics 23:947–2948.

Lee, J. C. 1992. *Anolis sagrei* in Florida: phenetics of a colonizing species III. West Indian and Middle American comparisons. Copeia 1992:942–954.

Lee, J. C. 2000. A Field Guide to the Amphibians and Reptiles of the Maya World. Cornell University Press pp. 402.

Legendre, P. and L. Legendre. 2012. Numerical Ecology. 3rd English Edition. Elsevier.

Lischer, H. E. L. and L. Excoffier. 2012. PGDSpider: An automated data conversion tool for connecting population genetics and genomics programs. Bioinformatics 28:298–299.

Lister, B. C. 1976a. The nature of niche expansion in West Indian *Anolis* lizards I: ecological consequences of reduced competition. Evolution 30:659–676.

Lister, B. C. 1976b. The nature of niche expansion in West Indian *Anolis* lizards II: evolutionary components. Evolution 30:677–692.

Logan, M. L., M. C. Duryea, O. R. Molnar, B. J. Kessler, and R. Calsbeek. 2016. Spatial variation in climate mediates gene flow across an island archipelago. Evolution 70:2395–2403.

Losos, J. B. 2009. Lizards in an Evolutionary Tree: Ecology and Adaptive Radiation of Anoles. University of California Press: Berkeley, CA.

Losos, J. B. 2011a. Convergence, adaptation, and constraint. Evolution 65:1827–1840.

Losos, J. B. 2011b. Seeing the forest for the trees: the limitations of phylogenies in comparative biology. Am. Nat. 177:709–727.

Losos, J. B., and K. de Queiroz. 1997. Evolutionary consequences of ecological release in Caribbean *Anolis* lizards. Biol. J. Linn. Soc. 61:459–483.

Losos, J.B., and D.L. Mahler. 2010. Adaptive radiation: The interaction of ecological opportunity, adaptation, and speciation. In: Evolution Since Darwin: The First 150 Years, pp381–420, eds Bell M, Futuyma DJ, Eanes WF, Levinton JS, Sinauer, Sunderland, MA.

Losos, J. B., D. J. Irschick, and T. W. Schoener. 1994. Adaptation and constraint in the evolution of specialization of Bahamian *Anolis* lizards. Evolution 48:1786–1798.

Losos, J. B., K. I. Warheitt, and T. W. Schoener. 1997. Adaptive differentiation following experimental island colonization in *Anolis* lizards. Nature 387: 70–73.

Losos, J. B., T. R. Jackman, A. Larson, K. de Queiroz, and L. Rodríguez-Schettino. 1998. Historical contingency and determinism in replicated adaptive radiations of island lizards. Science 279:2115–2118.

Lynn, W. G., and C. Grant. 1940. The Herpetology of Jamaica. Bull. Inst. Jamaica Sci. Series No. 1. The Institute of Jamaica.

Macey, J. R., A. Larson, N. B. Ananjeva, and T. J. Papenfuss. 1997. Evolutionary shifts in three major structural features of the mitochondrial genome among iguanian lizards. J. Mol. Evol. 44:660–674.

Macey, J. R., J. A. Schulte II, N. B. Ananjeva, A. Larson, N. Rastegar-Pouyani, S. M. Shammakov, and T. J. Papenfuss. 1998. Phylogenetic relationships among agamid lizards of the *Laudakia caucasia* species group: testing hypotheses of biogeographic fragmentation and an area cladogram for the Iranian Plateau. Mol. Phylogenet. Evol.10:118–131.

Mahler, D. L., T. Ingram, L. J. Revell, and J. B. Losos. 2013. Exceptional convergence on the macroevolutionary landscape in island lizard radiations. Science 341:292–295.

Malhotra, A., and R. S. Thorpe. 2000. The dynamics of natural selection and vicariance in the Dominican anole: patterns of within-island molecular and morphological divergence. Evolution 54:245–258.

Mantel, N. 1967. The detection of disease clustering and a generalized regression approach. Cancer Res. 27:209–220.

Marnocha, E., J. Pollinger, and T.B. Smith. 2011. Human-induced morphological shift in an island lizard. Evolutionary Applications 4:388–396.

Matos-Maraví, P., R. N. Aguila, C. Pena, J. Y. Miller, A. Sourakov, and N. Wahlberg. 2014. Causes of endemic radiation in the Caribbean: evidence from the historical biogeography and diversification of the butterfly genus *Calisto* (Nymphalidae: Satyrinae: Satyrini). BMC Evol. Biol. 14:199.

McCranie, J. R., and G. Köhler. 2015. The anoles of Honduras. Systematics, distribution, and conservation. Bull. Mus. Comp. Zool. SPS(1):1–292.

McCranie, J. R., L. D. Wilson, and G. Köhler. 2005. Amphibians and Reptiles of the Bay Islands and Cayos Cochinos, Honduras. Bibliomania! Salt Lake City, UT.

Muñoz, M. M., N. G. Crawford, T. J. McGreevy, N. J. Messana, R. D. Tarvin, L. J. Revell, R. M. Zandvliet, J. M. Hopwood, E. Mock, A. L. Schneider, and C. J. Schneider. 2013. Divergence in coloration and ecological speciation in the *Anolis marmoratus* species complex. Mol. Ecol. 22:2668–2682.

Nei, M. 1972. Genetic distance between populations. Am. Nat. 106:283–292.

Ng, J., and R. E. Glor. 2011. Genetic differentiation among populations of a Hispaniolan trunk anole that exhibit geographical variation in dewlap colour. Mol. Ecol. 20:4302–4317.

Nicholson, K. E., B. I. Crother, C. Guyer, and J. M. Savage. 2012. It is time for a new classification of anoles (Squamata: Dactyloidae). Zootaxa 3477:1–108.

Nosil, P., and T. E. Reimchen. 2005. Ecological opportunity and levels of morphological variance within freshwater stickleback populations. Biol. J. Linn. Soc. 86:297–308.

Oksanen, J., F. G. Blanchet, R. Kindt, P. Legendre, P. R. Minchin, R. B. O'Hara, G. L. Simpson, P. Solymos, M. H. H. Stevens, and H. Wagner. Vegan: community ecology package 2014. Available online: https://cran.r-project.org/web/packages/vegan/index.html (accessed on 4 August 2016).

Pagel, M. 1997. Inferring evolutionary processes from phylogenies. Zool. Scr. 26:331–348.

Pagel, M. 1999. Inferring the historical patterns of biological evolution. Nature 401:877–884.

Pante, E. and B. Simon-Bouhet. 2013. marmap: A package for importing, plotting and analyzing bathymetric and topographic data in R. PLoS ONE 8(9):e73051.

Paradis, A. E., S. Blomberg, B. Bolker, J. Claude, H. S. Cuong, R. Desper, G. Didier, B. Durand, J. Dutheil, and O. Gascuel. 2016. Package ape: Analyses of Phylogenetics and Evolution. Available from http://cran.r-project.org/web/packages/ape/.

Paradis, E. 2010. pegas: an R package for population genetics with an integrated-modular approach. Bioinformatics 26:419–420.

Paradis, E., J. Claude, and K. Strimmer. 2004. APE: analyses of phylogenetics and evolution in R language. Bioinformatics 20:289–290.

Parent, C. E., and B. J. Crespi. 2009. Ecological opportunity in adaptive radiation of Galapagos endemic land snails. Am. Nat. 174:898–905.

Poe, S. 2004. Phylogeny of anoles. Herpetol. Monographs 18:37–89.

Poe, S., J. R. Goheen, and E. P. Hulebak. 2007. Convergent exaptation and adaptation in solitary island lizards. Proc. Royal Soc. London Series B 274:2231–2237.

Poe, S., A Nieto-Montes de Oca, O. Torres-Carvajal, K. De Queiroz, J. A. Velasco, B. Truett, L.N. Gray, M.J. Ryan, G. Köhler, F. Ayala-Verla, and I. Latella. 2017. A phylogenetic, biogeographic, and taxonomic study of all extant species of *Anolis* (Squamata: Iguanidae). Syst. Biol. 66:663–697.

Price, T., I. J. Lovette, E. Bermingham, H. L. Gibbs, and A. D. Richman. 2000. The imprint of history on communities of North American and Asian warblers. American Naturalist 156:354–367.

Price, T. D., A. B. Phillimore, M. Awodey, and R. Hudson. 2010. Ecological and geographical influences on the allopatric phase of island speciation. *In* P. R. Grant and B. R. Grant, eds. In Search of the Causes of Evolution: From Field Observations to Mechanisms. Princeton Univ. Press, Princeton, NJ.

Pritchard, J. K., M. Stephens, and P. Donnelly. 2000. Inference of population structure using multilocus genotype data. Genetics 155:945–959.

R Development Team. 2016. R: a language and environment for statistical computing. R Foundation for Statistical Computing, Vienna, Austria. Available from https://www.R-project.org.

Ramasamy, R. K., S. Ramasamy, B. B. Bindroo, and V. G. Naik. 2014. STRUCTURE PLOT: a program for drawing elegant STRUCTURE bar plots in user friendly interface. Springerplus 2014 Aug 13:3:431.

Rambaut, A., M. A. Suchard, D. Xie, A. J. Drummond. 2013. Tracer v1.5, Available from http://beast.bio.ed.ac.uk/Tracer.

Revell, L. J. 2009. Size–correction and principal components for interspecific comparative studies. Evolution 63:3258–3268.

Revell, L. J. 2012. phytools: an R package for phylogenetic comparative biology (and other things). Methods Ecol. Evol. 3:217–223.

Revell, L. J. 2013. Two new graphical methods for mapping trait evolution on phylogenies. Methods Ecol. Evol. 4:754–759.

Revell, L. J., L. J. Harmon, R. B. Langerhans, and J. J. Kolbe. 2007. A phylogenetic approach to determining the importance of constraint on phenotypic evolution in the neotropical lizard *Anolis cristatellus*. Evol. Ecol. Res. 9:261–282.

Riddle, B. R., M. N. Dawson, E. A. Hadly, D. J. Hafner, M. J. Hickerson, S. J. Mantooth, and A. D. Yoder. 2008. The role of molecular genetics in sculpting the future of integrative biogeography. Prog. Phys. Geogr. 32:173–202.

Rodríguez, A., M. Vences, B. Nevado, A. Machordom, and E. Verheyen. 2010. Biogeographic origin and radiation of Cuban *Eleutherodacytlus* frogs of the *auriculatus* species group,

inferred from mitochondrial and nuclear gene sequences. Mol. Phylogenet. Evol. 54:179–186.

Rodríguez-Robles, J. A., T. Jezkova, and M. A. García. 2007. Evolutionary relationships and historical biogeography of *Anolis desechensis* and *Anolis monensis*, two lizards endemic to small islands in the eastern Caribbean Sea. J. Biogeogr. 34:1546–1558.

Rodríguez-Schettino, L. 1999. The Iguanid Lizards of Cuba. University Press of Florida 428pgs.

Rodríguez-Schettino, L., J. B. Losos, P. E. Hertz, K. de Queiroz, A. R. Chamizo, M. Leal, and V. Rivalta. 2010. The anoles of Soroa: aspects of their ecological relationships. Breviora 520:1–21.

Román-Palacios, C., J. Tavera, M. d. R. Castañeda. 2018. When did anoles diverge? An analysis of multiple dating strategies. Mol. Phylogenet. Evol. 127: 655-668.

RStudio Team. 2016. RStudio: Integrated Development Environment for R. Available at http://www.rstudio.com.

Ruibal, R. 1964. An annotated checklist and key to the anoline lizards of Cuba. Bull. Mus. Comp. Zool. 130:473–520.

Russello, M. A., M. D. Waterhouse, P. D. Etter, and E. A. Johnson. 2015. From promise to practice: pairing non-invasive sampling with genomics in conservation. PeerJ 3:e1106.

Schluter, D. 2000. The Ecology of Adaptive Radiation. Oxford University Press, Oxford, UK.

Schnute, J. T., A. Couture-Beil, R. Haigh, and A. R. Kronlund. 2013. PBSmodelling 2.65: 545 User's guide. Canadian Technical Report of Fisheries and Aquatic Sciences 2674: viii + 546 194 p.

Schoener, T. W. 1969. Size patterns in West Indian *Anolis* lizards: I. Size and species diversity. Syst Zool 18: 386–401.

Schoener, T. W. and A. Schoener. 1980. Densities, sex ratios, and population structure in four species of Bahamian *Anolis* lizards. J. Anim. Ecol. 49: 19–53.

Schoener, T. W. and A. Schoener. 1983. The time to extinction of a colonizing propagule of lizards increases with island area. Nature 302: 332–334.

Schoener, T. W., and D. A. Spiller. 2010. Trophic cascades on islands. Pp. 179–202 in J. Terborgh and J. A. Estes, eds., Trophic Cascades: Predators, Prey, and the Changing Dynamics of Nature. Island Press, Washington.

Schoener, T. W., J. J. Kolbe, M. Leal, J. B. Losos, and D. A. Spiller. 2017. A multigenerational field experiment on eco-evolutionary dynamics of the influential lizard *Anolis sagrei*: a mid-term report. Copeia 105:543–549.

Schwartz, A. 1968. Geographic variation in *Anolis distichus* Cope (Lacertilia, Iguanidae) in the Bahama Islands and Hispaniola. Bull. Mus. Comp. Zool. Harvard 137:255–309.

Schwartz, A., and R. Thomas. 1975. A check-list of West Indian amphibians and reptiles. Special Publication. Carnegie Mus. Nat. Hist. Pittsburgh 1:1–216.

Sexton, O. J., and K. M. Brown. 1977. The reproductive cycle of an iguanid lizard, Anolis sagrei, from Belize. J. Nat. Hist.11:241–250.

Sherratt, E., M. d. R. Castañeda, R. J. Garwood, D. L. Mahler, T. J. Sanger, A. Herrel, K de Queiroz, and J. B. Losos. 2015. Amber fossils demonstrate deep-time stability of Caribbean lizard communities. Proc. Natl. Acad. Sci. USA 112:9961–9966.

Smith, H. M., and W. L. Burger. 1949. A new subspecies of *Anolis sagrei* from the Atlantic coast of tropical America. Anal. Inst. Biol. 10:407–410.

Soetaert, K. 2013. plot3D: Plotting multi-dimensional data. R package version 1.0.

Stamatakis, A. 2006. RaxML-VI-HPC: maximum likelihood-based phylogenetic analyses with thousands of taxa and mixed models. Bioinformatics 22:2688–2690.

Stamps, J. A., and R. M. Andrews. 1992. Estimating asymptotic size using the largest individuals per sample. Oecologia 92:503–512.

Stankiewicz, J., C. Thiart, J. C. Masters, and M. J. de Wit. 2006. Did lemurs have sweepstake tickets? An exploration of Simpson's model for the colonization of Madagascar by mammals. J. Biogeogr. 33:221–235.

Stroud, J. T., and J. B. Losos. 2016. Ecological opportunity and adaptive radiation. Ann. Rev. Ecol. Evol. Syst. 47:507–532.

Stroud, J. T., S. T. Giery, and M. E. Outerbridge. 2017. Establishment of Anolis sagrei on Bermuda represents a novel ecological threat to Critically Endangered Bermuda skinks (*Plestiodon longirostris*). Biol. Invasions 19:1723–1731.

Stuart, Y. E.; T. S. Campbell, P. A. Hohenlohe, R. G. Reynolds, L. J. Revell, J. B. Losos 2014. Rapid evolution of a native species following invasion by a congener. Science 346:463–466.

Takezaki, N., and M. Nei. 1996. Genetic distances and reconstruction of phylogenetic trees from microsatellite DNA. Genetics 144:389–399.

Tamura, K., G. Stecher, D. Peterson, A. Filipski, S. Kumar. 2013. MEGA6: Molecular evolutionary genetics analysis version 6.0. Mol. Evol. Biol. 30:2725–2729.

Taylor, D. J, and W. H. Piel. 2004. An assessment of accuracy, error, and conflict with support values from genome-scale phylogenetic data. Mol. Biol. Evol. 21:1534–1537.

Thorpe, R. S., A. Barlow, A. Malhotra, and Y. Surget-Groba. 2015. Widespread parallel population adaptation to climate variation across a radiation: implications for adaptation to climate change. Mol. Ecol. 24:1019–1030.

Thorpe, R. S., Y. Surget-Groba, and H. Johansson. 2008. The relative importance of ecology and geographic isolation for speciation in anoles. Phil. Trans. Roy. Soc. Lond. B 363:3071–3081.

Thorpe, R. S. 2017. Predictability in evolution: adaptation of the Bonaire anole (*Anolis bonairensis*) to an extreme environment. PLOS ONE 12(5): e0176434.

Tollis, M., G. Ausubel, D. Ghimire, and S. Boissinot. 2012. Multi-locus phylogeographic and population genetic analysis of *Anolis carolinensis*: historical demography of a genomic model species. PLoS ONE 7:e38474.

Uetz, P., and J. Hošek. 2016. The Reptile Database, http://www.reptile-database.org, accessed August 13, 2016.

Underwood, G., and E. E. Williams. 1959. The anoline lizards of Jamaica. Bull. Inst. Jamaica Sci. Ser. 9:1–48.

Vanhooydonck, B., A. Herrel, J. J. Meyers, and D. J. Irschick. 2009. What determines dewlap diversity in *Anolis* lizards? An among-island comparison. J. Evol. Biol. 22:293–305.

Venables, W. N. and B. D. Ripley. 2002. Modern Applied Statistics with S. Fourth Edition. Springer, New York.

Weiss, A. C. and S. B. Hedges. 2007. Molecular phylogeny and biogeography of the Antillean geckos *Phyllodactylus wirshingi*,*Tarentola americana*, and *Hemidactylus haitianus* (Reptilia, Squamata). Mol. Phylogenet. Evol. 45:409–416.

Wellborn, G. A. and R. B. Langerhans. 2015. Ecological opportunity and the adaptive diversification of lineages. Ecol. Evol. 5:176–195.

Wickham, H. 2009. ggplot2: Elegant Graphics for Data Analysis. Springer-Verlag, New York.

Williams, E. E. 1969. The ecology of colonization as seen in the zoogeography of anoline lizards on small islands. Quart. Rev. Biol. 44:345–389.

Williams, E. E. 1983. Ecomorphs, faunas, island size, and diverse end points in island radiations of *Anolis*. Pp. 326–370 *in* R. B. Huey, E. R. Pianka, and T. W. Schoener, eds. Lizard ecology: studies of a model organism. Harvard Univ. Press, Cambridge.

Winchell, K.M., R.G. Reynolds, S. Prado-Irwin, A.R. Puente-Rolón, and L.J. Revell. 2016. Phenotypic shifts in urban areas in the tropical lizard *Anolis cristatellus*. Evolution 70:1009–1022

Wollenberg, K. C., I. J. Wang, R. E. Glor, and J. B. Losos. 2013. Determinism in the diversification of Hispaniolan trunk-ground anoles (*Anolis cybotes* species complex). Evolution 67:3175–3190.

Wright, S. J. 1981. Extinction-mediated competition: the *Anolis* lizards and insectivorous birds of the West Indies. Am. Nat. 117: 181–192.

Yoder, A. D., and M. D. Nowak. 2006. Has vicariance or dispersal been the predominant biogeographic force in Madagascar? Only time will tell. Ann. Rev. Ecol. Evol. Syst. 37:405–431.

Yoder, J. B., E. Clancey, S. Des Roches, J. M. Eastman, L. Gentry, W. Godsoe, T. J. Hagey, D. Jochimsen, B. P. Oswald, J. Robertson, B. A. J. Sarver, J. J. Schenk, S. F. Spear, and L. J. Harmon. 2010. Ecological opportunity and the origin of adaptive radiations. J. Evol. Biol. 23:1581–1596.

Figure 1. a) Hypothesized spread of *A. sagrei* diaspora from an ancestral range in Cuba from Williams (1969), reprinted with permission. b) Our interpretation of the native range of *A. sagrei* across the Caribbean Basin (in dark gray). Note that it has been considered unclear whether populations on Jamaica and in Mesoamerica are native or anthropogenically introduced. Proposed subspecies are shown (after Schwartz and Thomas 1975), and the other species within the *sagrei* species group are shown in western Cuba. Arrows show hypothetical dispersal patterns in the *sagrei* group is overlaid on the map. Geographic points mentioned in the text are labeled. The photo, taken by RGR, is of a male *A. sagrei* from Conception Island, Bahamas.

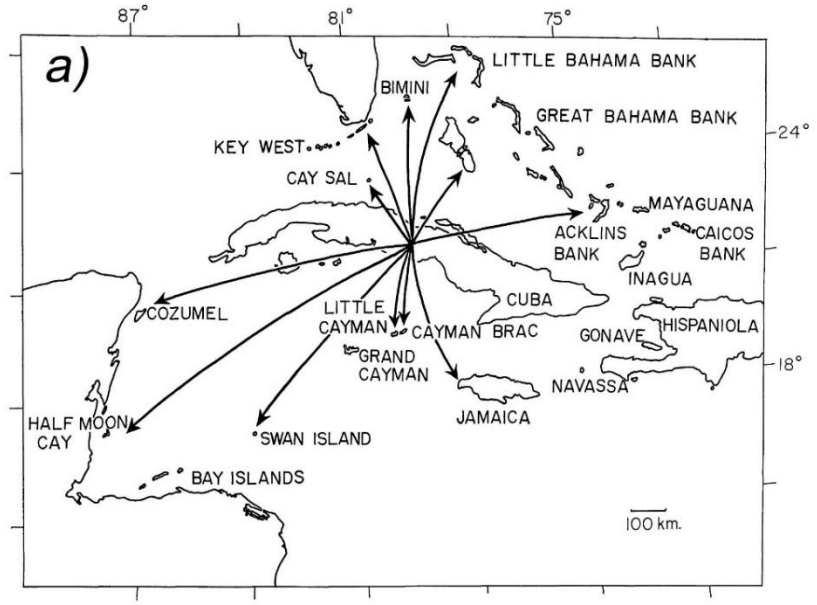
a)
87°
81°
75°
24°
18°
LITTLE BAHAMA BANK
BIMINI
GREAT BAHAMA BANK
KEY WEST
CAY SAL
MAYAGUANA
ACKLINS BANK
CAICOS BANK
INAGUA
CUBA
COZUMEL
LITTLE CAYMAN
CAYMAN BRAC
GONAVE
HISPANIOLA
GRAND CAYMAN
NAVASSA
JAMAICA
HALF MOON CAY
SWAN ISLAND
BAY ISLANDS
100 km.

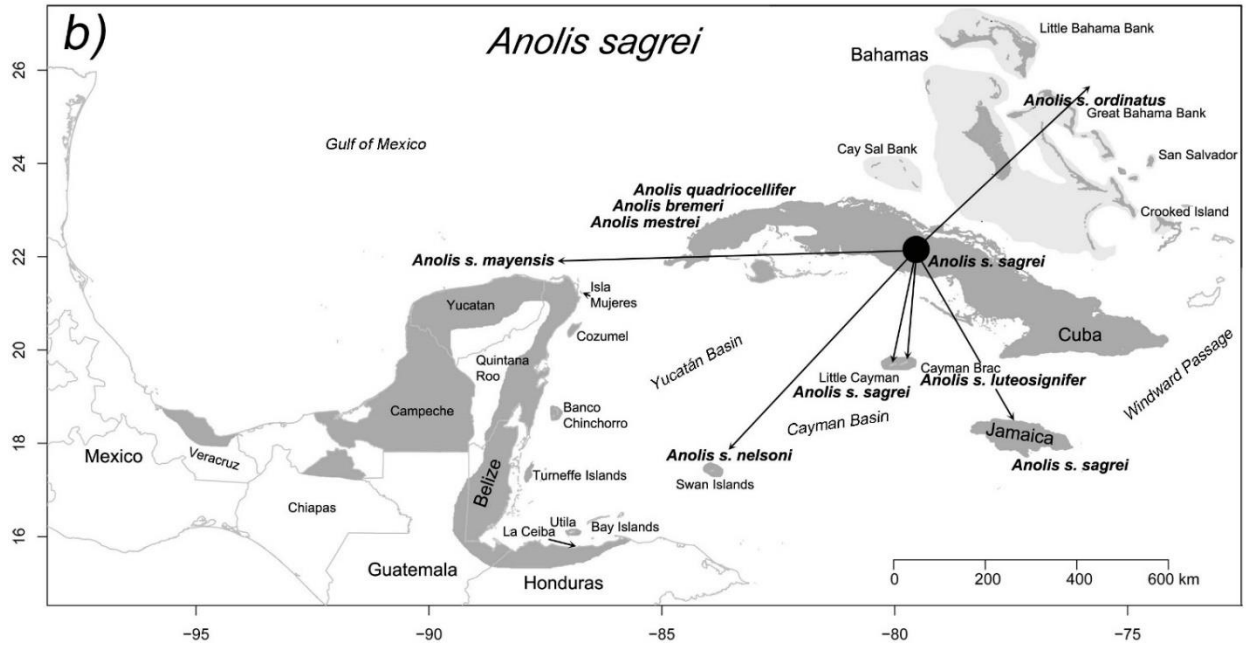
b)
Anolis sagrei
Bahamas
Little Bahama Bank
Anolis s. ordinatus
Great Bahama Bank
Gulf of Mexico
Cay Sal Bank
San Salvador
Anolis quadriocellifer
Anolis bremeri
Anolis mestrei
Crooked Island
Anolis s. mayensis
Anolis s. sagrei
Isla Mujeres
Yucatan
Cozumel
Cuba
Quintana Roo
Yucatán Basin
Little Cayman
Cayman Brac
Anolis s. sagrei
Anolis s. luteosignifer
Windward Passage
Campeche
Banco Chinchorro
Cayman Basin
Jamaica
Mexico
Veracruz
Anolis s. nelsoni
Anolis s. sagrei
Turneffe Islands
Swan Islands
Belize
Chiapas
Utila
Bay Islands
La Ceiba
Guatemala
Honduras
0
200
400
600 km
26
24
22
20
18
16
−95
−90
−85
−80
−75

1435

Figure 2. a) Map of sampling locations in this study, color-coded by the mtDNA clade to which they belong. b) Time-calibrated mtDNA gene tree for *Anolis sagrei* from BEAST with nodal support shown. c) Neighbor-joining SNP tree for a subset of samples from across the range of *A. sagrei*. Tips are color-coded by mtDNA clade to show correspondence between mtDNA and nucDNA phylogenetic inferences. Map rendered in the R package *marmap* (Pante and Simon-Bouhet 2013) from NOAA bathymetric data at a resolution of 1 arc minute.

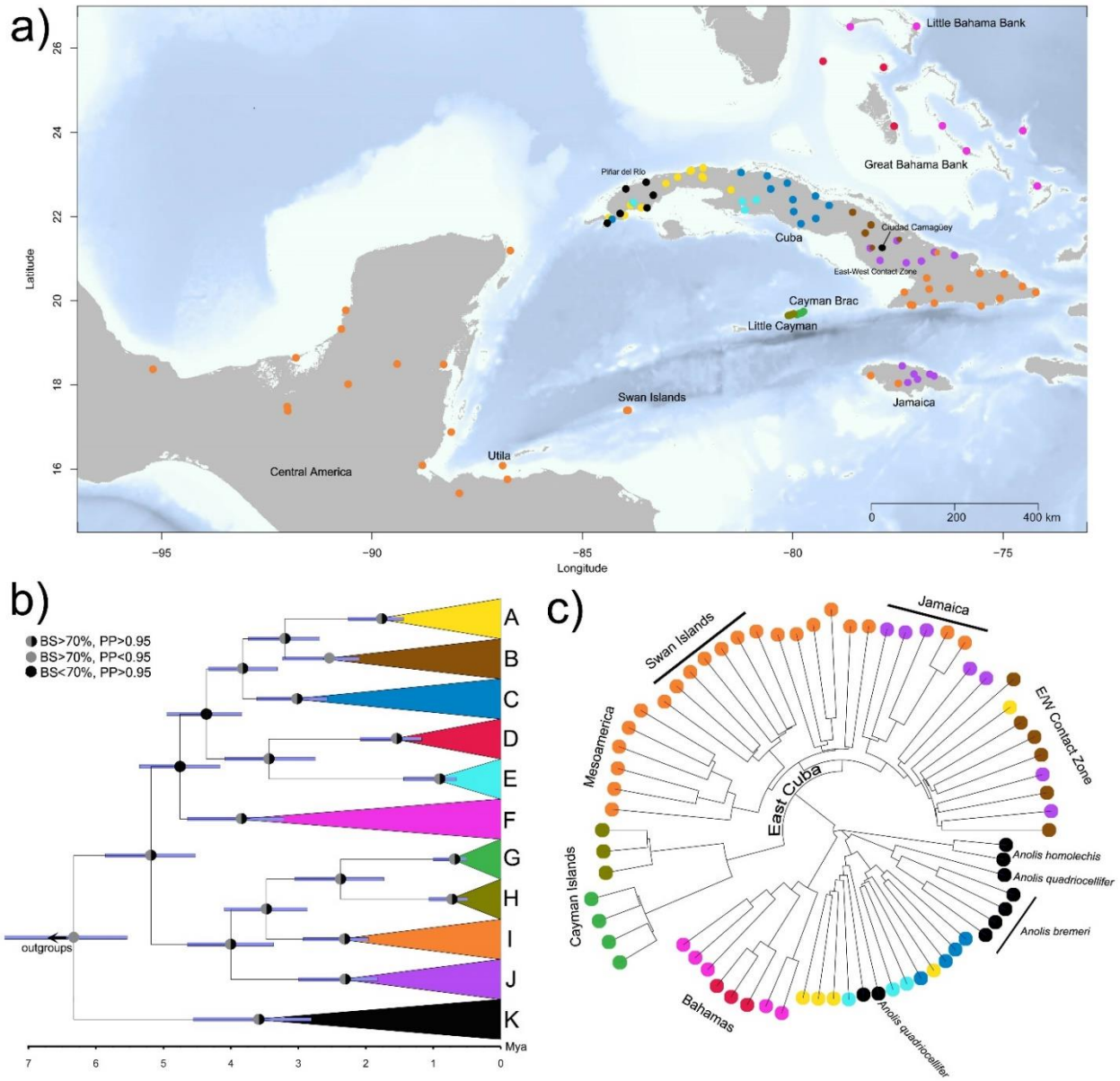

Figure 3. Relationships between genetic and geographic distance in *Anolis sagrei* across the Caribbean Basin, showing a) an isolation-by-distance (IBD) plot for the mtDNA dataset, b) IBD for the nuclear dataset, c) a regression with the relationship between the dependent matrix of SNP distance on the independent matrix of mtDNA distance, and d) a visualization of the matrices from the multiple matrix regression (partial mantel test) showing the relationship between SNP and mtDNA distances when controlling for geographic distance. Note that mtDNA distance (axis z) is less dependent on geographic distance (axis y), while SNP distance (axis x) has a greater correlation with geographic distance (axis y).

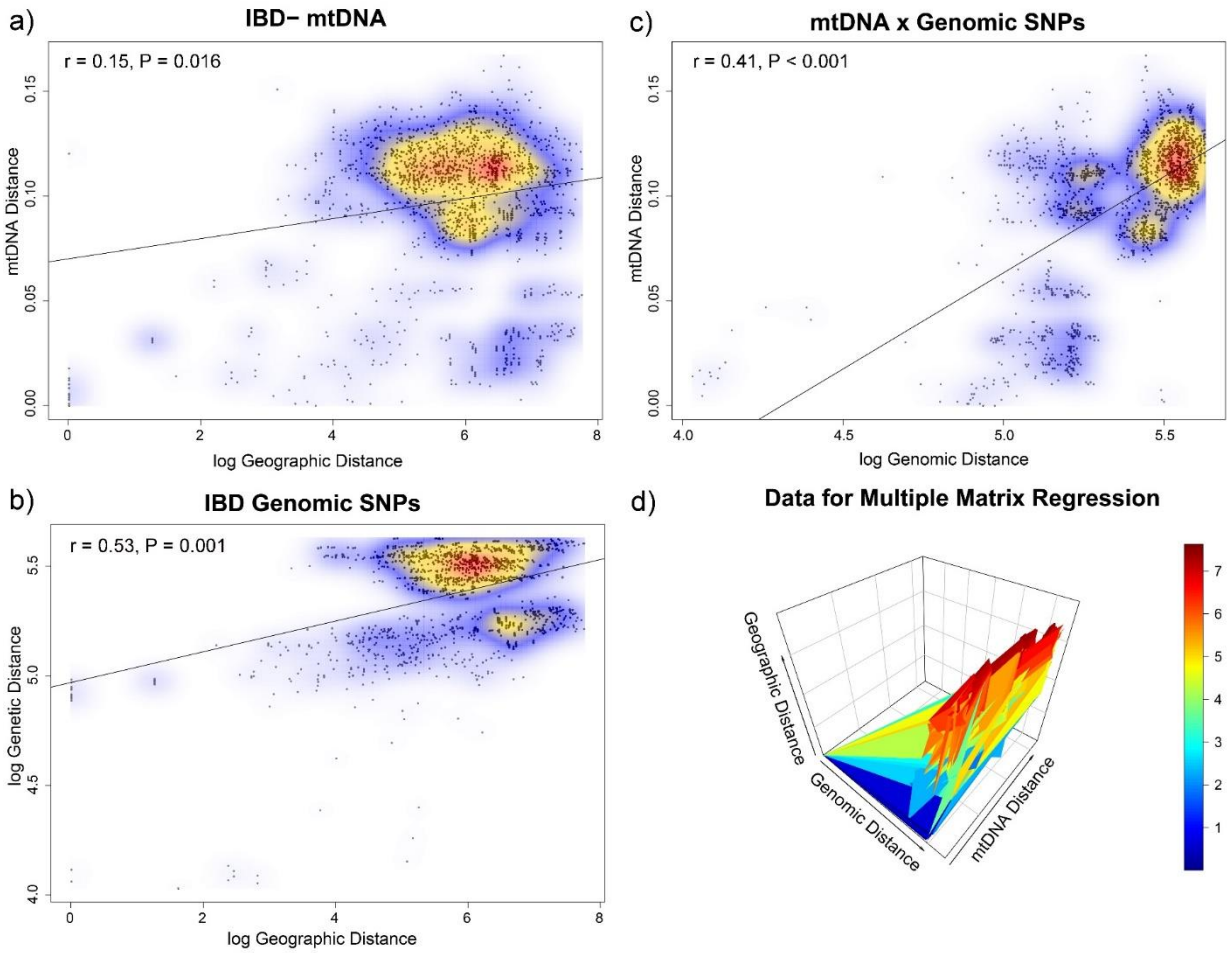

Figure 4. Phylogenetic network of 16,382 SNP loci among 69 representative samples from across the range of *Anolis sagrei*. Major nodes and nodes of interest with > 70% bootstrap support are labeled. Branches are colored according to their genetic cluster assignment determined using STRUCTURE, with other members of the *A. sagrei* superspecies (*A. bremeri* and *A. quadriocellifer*) and the *A. sagrei* series (*A. homolechis*) colored in black.

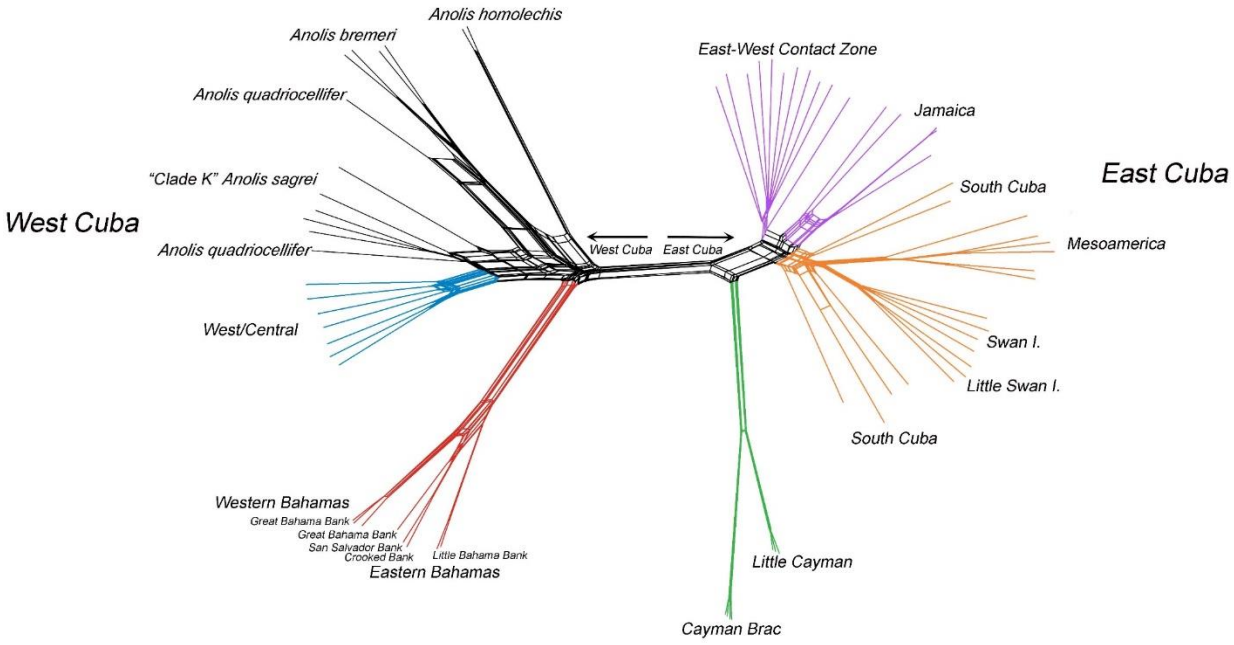

Figure 5. Map showing genetic cluster assignments from a) 1000 SNP loci using the Bayesian clustering algorithm STRUCTURE, and b) 31,702 SNP loci using Discriminant Analysis of Principal Components.

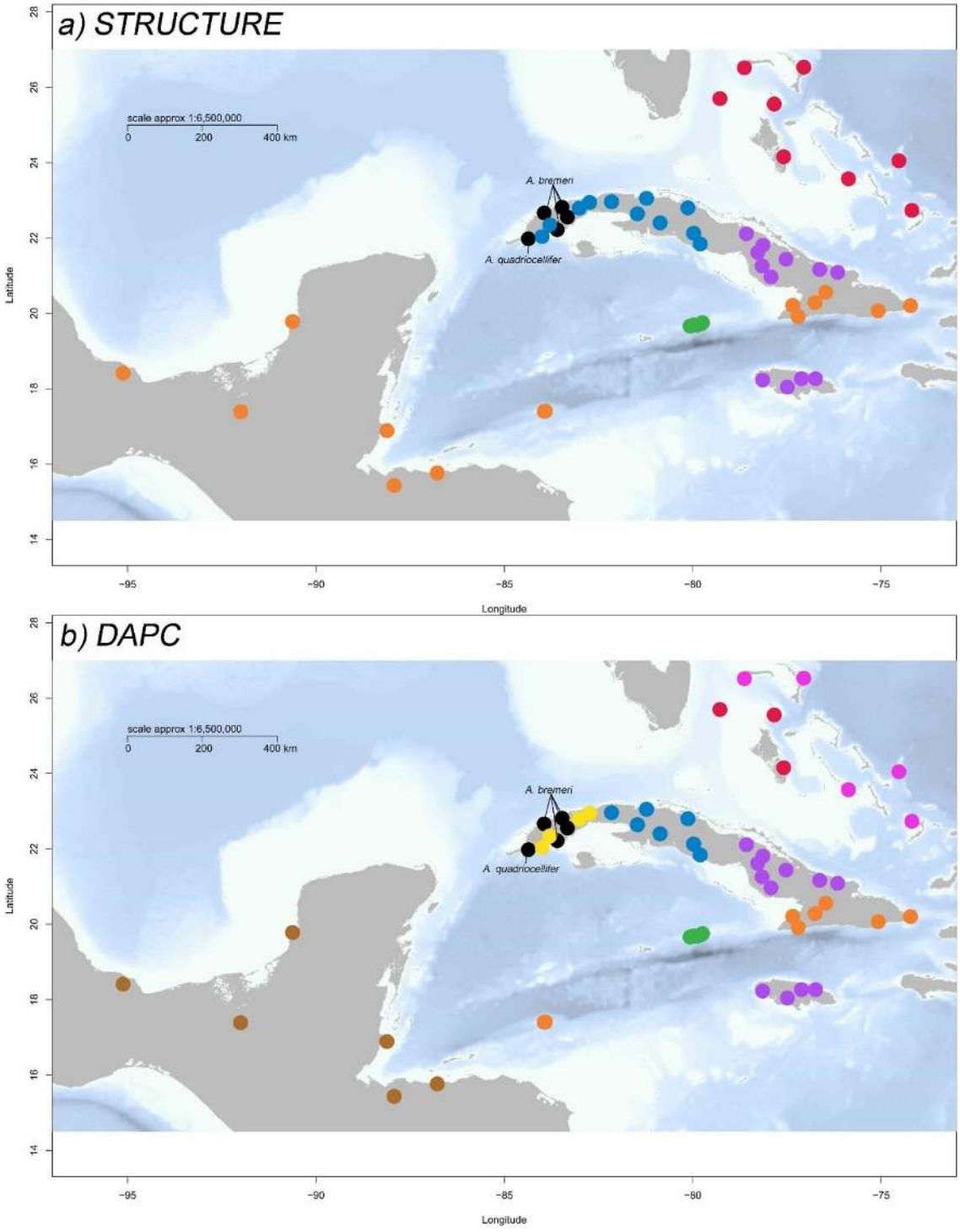

Figure 6. Distributions of snout-vent length and residuals from size-corrected quantitative trait mean and variance in Cuban and diaspora groupings of *A. sagrei*. Each plot shows denstity plots of residual trait mean and variance in Cuban (red) and diaspora (blue) populations. Dotted lines are the mean for each group. The table lists values for mean and variance for each trait as well as results from a Levene's test of trait variance. Significant values are in bold.

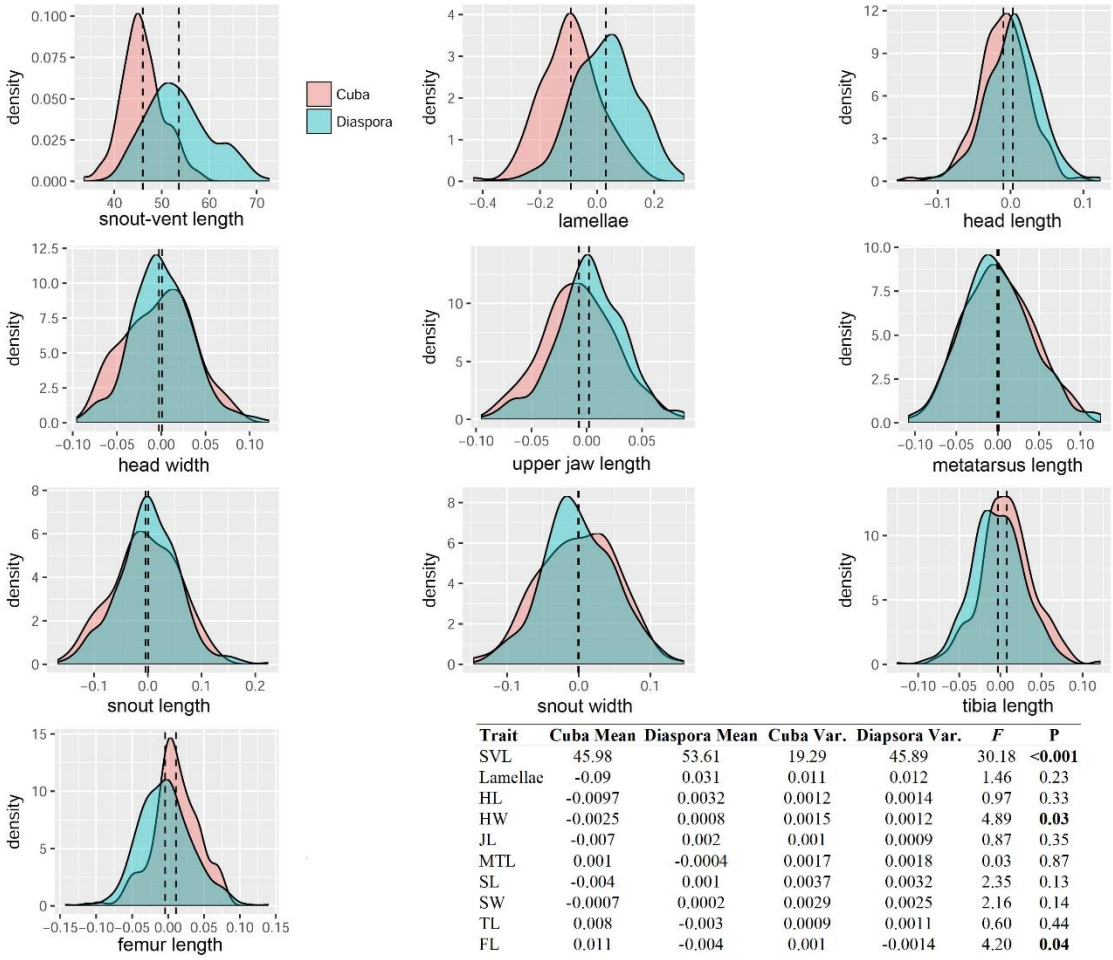

Trait	Cuba Mean	Diaspora Mean	Cuba Var.	Diapsora Var.	*F*	P
SVL	45.98	53.61	19.29	45.89	30.18	**<0.001**
Lamellae	-0.09	0.031	0.011	0.012	1.46	0.23
HL	-0.0097	0.0032	0.0012	0.0014	0.97	0.33
HW	-0.0025	0.0008	0.0015	0.0012	4.89	**0.03**
JL	-0.007	0.002	0.001	0.0009	0.87	0.35
MTL	0.001	-0.0004	0.0017	0.0018	0.03	0.87
SL	-0.004	0.001	0.0037	0.0032	2.35	0.13
SW	-0.0007	0.0002	0.0029	0.0025	2.16	0.14
TL	0.008	-0.003	0.0009	0.0011	0.60	0.44
FL	0.011	-0.004	0.001	-0.0014	4.20	**0.04**

1475 **Figure 7.** a) PCA of Cuba versus diaspora populations (including Jamaican populations as diaspora). b) Discriminant function analysis indicates good ability to diagnose Cuban and diaspora populations based on quantitative traits. All points represent population means.

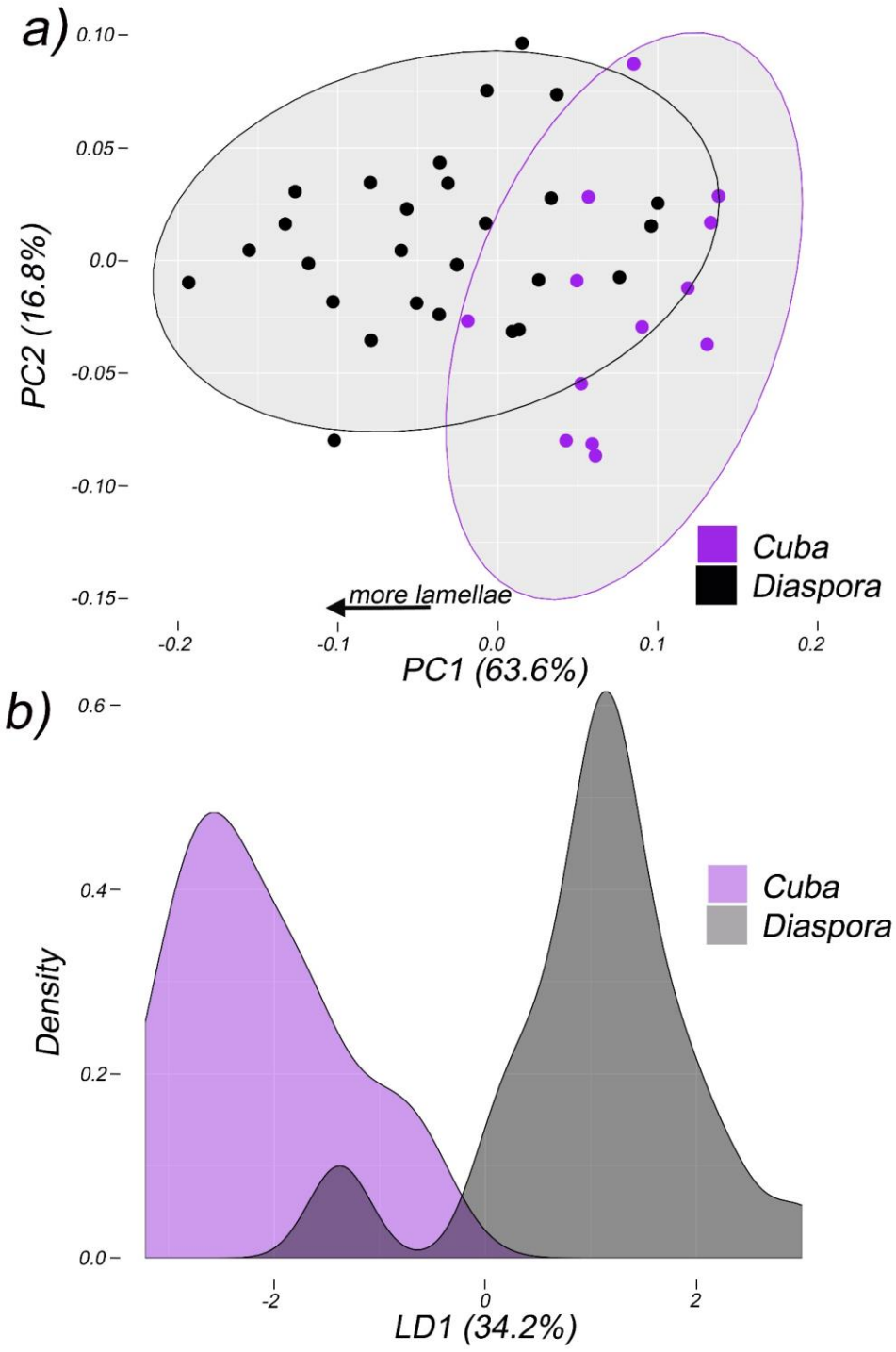

Figure 8. Boxplots showing **A)** body size (SVL) on top and **B)** size-corrected lamella number on bottom for regional groupings of *A. sagrei* in order of mean body size of each regional population. Note that Jamaican *A. sagrei* are recent diaspora (including anthropogenic introductions from Cuba) and that Jamaica has six other native species of anoles.

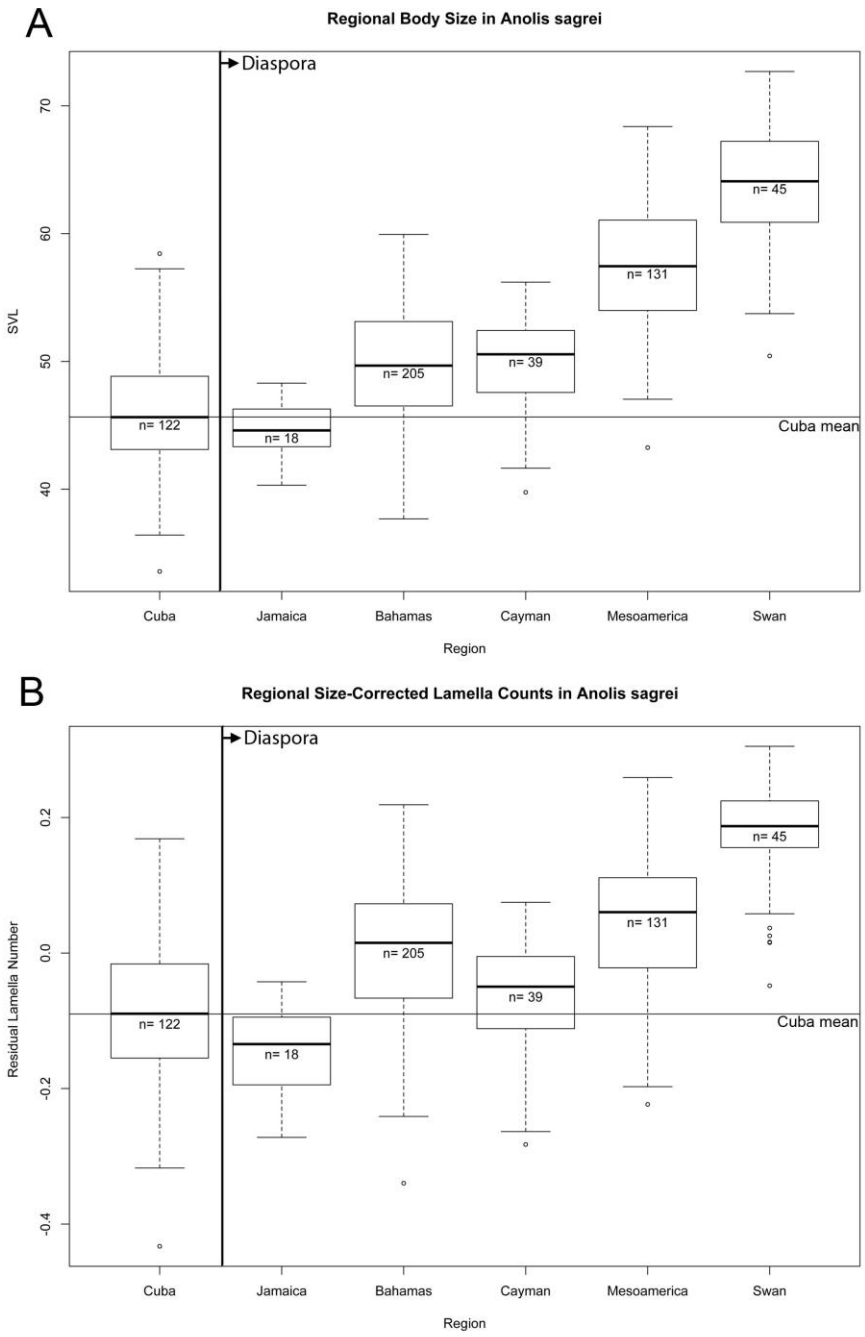

Figure 9. a) PCA by region. b) Discriminant function analysis by region. Populations from the Bahamas (red) that cluster with Cuba (purple) are from the Little Bahama Bank, where individuals tend to be smaller in body size than other Bahamian populations. All points represent population means, and 95% confidence ellipses are shown for groups with more than two populations.

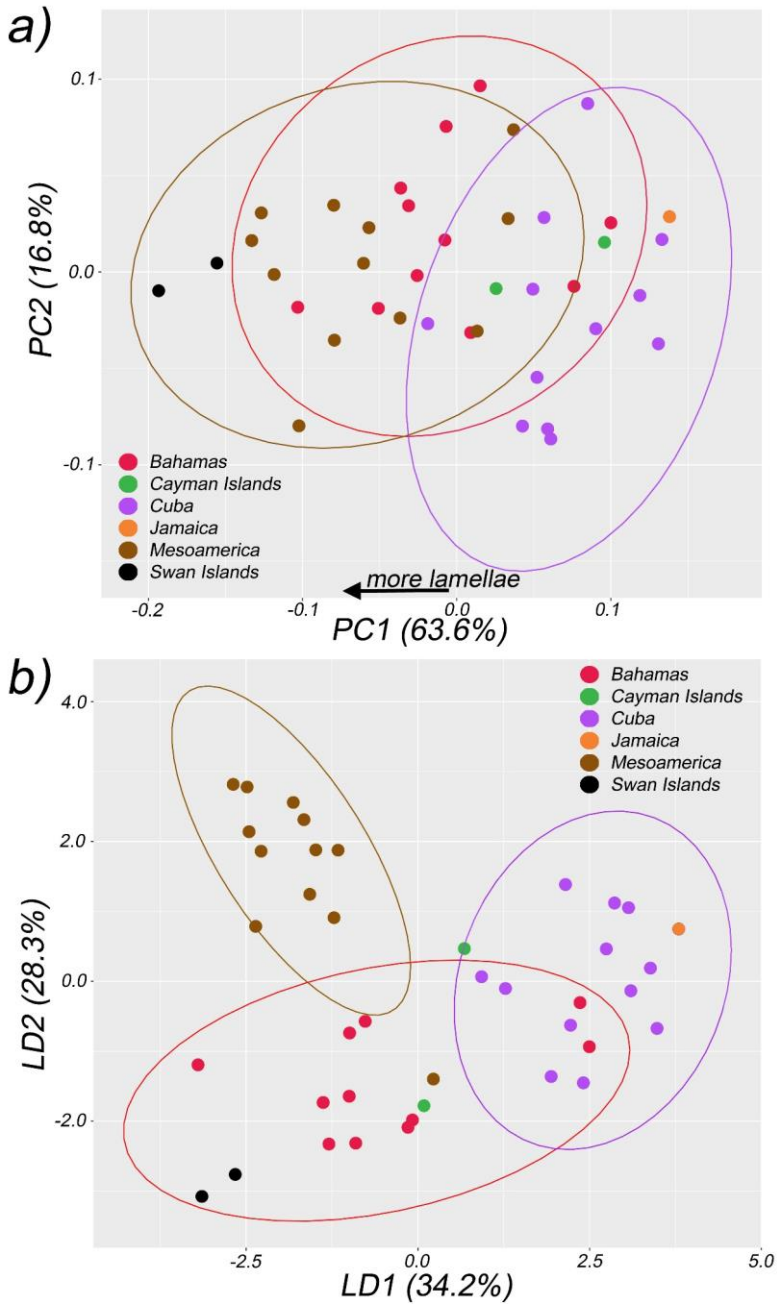

Table 1. Mitochondrial DNA summary statistics for *Anolis sagrei* clades. *N* = number of individuals, *n* = number of haplotypes, *S* = number of segregating sites, *h* = haplotype diversity ± SD, π = nucleotide diversity ± SD. Coalescent times, Highest Posterior Density (HPD) and Posterior Probabilities are from a molecular-clock calibrated analysis in Beast, while Bootstrap percentages are from a maximum-likelihood (ML) analysis in RaXML.

Clade	*N*	*n*	*S*	*h*	π	Mean Coalescent Time (Mya)	95% HPD (Mya)	Posterior Probability	Bootstrap %
A	35	31	44	0.99±0.01	0.006±0.003	3.2	3.7, 2.7	1	93
B	6	6	13	1.00±0.09	0.005±0.003	3.2	3.7, 2.7	1	93
C	7	5	15	0.90±0.10	0.005±0.003	3.8	4.3, 3.3	1	99
D	23	8	9	0.82±0.06	0.002±0.001	3.4	4.1, 2.8	1	86
E	33	18	26	0.91±0.03	0.004±0.002	3.4	4.1, 2.8	1	86
F	28	25	53	0.99±0.01	0.009±0.005	4.8	5.4, 4.2	0.99	51
G	8	4	10	0.75±0.14	0.004±0.003	2.4	3.1, 1.7	1	100
H	4	2	1	0.67±0.20	0.001±0.001	2.4	3.1, 1.7	1	100
I	11	5	9	0.71±0.14	0.002±0.001	3.5	4.1, 2.9	0.96	92
J	7	4	7	0.86±0.10	0.002±0.001	4.0	4.7, 3.4	1	100
K	7	6	13	0.95±0.09	0.004±0.003	6.4	7.4, 5.5	0.42	87

Abstract (336 words); Text (11819 words); Acknowledgements (244 words); References (185 count; 4801 words); Tables (5); Figures (9); Supplementary information (16 Figures, 7 Tables)

Table 2. Results from Mantel tests for correlation between geographic, genetic, and morphological distance pairings. Genetic distances are calculated as the Cavalli-Sforza chord distance (SNPs) or Nei's pairwise distance (mtDNA). Multiple matrix regression is a partial Mantel test for correlation between two matrices while controlling for a third.

Dataset and Method	**↓Dependent | Independent→**	**Geographic Distance**	**mtDNA Distance**
Genetic Data			
Mantel test	mtDNA Distance	r =0.15, *P* = 0.016	–
Mantel test	SNP Distance	r =0.41, *P* < 0.001*	r =0.53, *P* = 0.001*
Multiple Matrix Regression	SNP Distance	–	r =0.52, *P* = 0.001*
Morphometric Data			
Mantel test	PC1	r = 0.18, *P* = 0.001*	–
Mantel test	PC2	r = -0.06, *P* = 0.85	–
Mantel test	PC3	r = 0.02, *P* = 0.33	–

* Significant at *P* < 0.05

1500

Table 3. Clustering analyses for the SNP datasets. Also see Figs. 4 and 5. Datasets refer to inclusive (= "all", including outgroups) and exclusive (*Anolis sagrei* sensu stricto) SNP genotype datasets.

Method	Dataset	n	*K*	PCs	Clusters
DAPC	All	69	5	5	Bahamas, West Cuba, East Cuba, Caymans, Other Species
	A. sagrei	61	3	2	West Cuba, East Cuba, Caymans
	West Cuba	20	4	3	West Cuba, West/Central Cuba, West Bahamas, East Bahamas,
	East Cuba	34	3	2	East Cuba/Swan I., Mesoamerica, East Cuba/Jamaica
STRUCTURE	All	–	–	–	–
	A. sagrei	61	2	–	ECuba, WCuba
			4	–	ECuba, WCuba, Caymans, Bahamas
	West Cuba	20	2	–	WCuba, Bahamas
	East Cuba	34	2	–	E/C Cuba/Swan Islands/Central America, E/S Cuba/Jamaica
			5	–	Swan Islands, E/C Cuba, Central America, Jamaica, E/S Cuba

Table 4. Analyses of quantitative traits for *Anolis sagrei* from Cuban and Diaspora groupings. Results from a MANOVA analysis based on orthogonalized axes from a PCA analysis, as well as raw residuals from QT regression on SVL, indicate differences between Cuban and Diaspora groupings. Individual Welch's two-sample t-tests performed on size-corrected residuals of population means indicate that Diaspora populations have significantly more lamellae and larger body sizes than Cuban populations after a Benjamini-Hochberg correction (Padj). ANOVA of traits (SVL and size-corrected lamellae) from regional groupings (Cuba, Bahamas, Caymans, Mesoamerica, Swan Islands) show significant differences among groups. Post-hoc Tukey analyses show that all Diaspora regional groupings differ significantly from Cuba populations for both traits (Fig. S15).

MANOVA		**Wilks**	**F**	**P**	
	All PCs	0.26	9.5	<0.001	
	QT residuals	0.62	37.0	<0.001	
T-Tests	**Trait**	**t**	**d.f.**	**P**	**Padj**
	FL	2.06	37.9	0.05*	0.12
	HL	-1.67	28.3	0.11	0.22
	HW	-0.86	20.1	0.40	0.57
	JL	-1.39	20.7	0.18	0.30
	Lamellae	-6.53	36.5	<0.001*	<0.001*
	MTL	0.10	27.9	0.91	0.79
	SL	0.29	19.1	0.78	0.79
	SW	0.39	19.8	0.70	0.79
	TL	2.46	31.4	0.02*	0.06
	SVL	6.24	37.1	<0.001*	<0.001*

ANOVA	**Trait**	**d.f.**	**SS**	**F**	**P**
	FL	5	0.10	17.6	<0.001*
	HL	5	0.04	5.8	<0.001*
	HW	5	0.06	10.1	<0.001*

JL	5	0.03	5.5	<0.001*
Lamellae	5	3.00	65.9	<0.001*
MTL	5	0.04	4.4	<0.001*
SL	5	0.13	8.1	<0.001*
SW	5	0.87	7.1	<0.001*
TL	5	0.03	5.2	<0.001*
SVL	5	16433	157.1	<0.001*

*significant at $P \leq 0.05$

1520 **Table 5.** Results of discriminate function analysis for the morphometric dataset, followed by using LDA axes to predict group membership yielding the proportion of correct assignments (PoCA). Groupings are *a priori* groupings, and LD1 and LD2 are the intragroup variance explained by each of the first two LDA axes. The data are population means, not individual-animal data. P-values represent results from a 1-sided exact binomial test, where the alternative hypothesis is that the PoCA observed is higher than expected by chance.

Grouping	# groups	LD1	LD2	PoCA	P-value
Subspecies	5	39.3	33.2	0.90	<0.001*
Region	7	34.2	28.3	0.88	<0.001*
mtDNA	9	31.9	28.1	0.85	<0.001*
STRUCTURE	6	39.3	23	0.85	<0.001*

DAPC	7	37.1	21.6	0.80	<0.001*
Cuba/Diaspora	2	100	–	0.93	<0.001*

* Significant at $P < 0.05$